Distribution Agreement

In presenting this thesis as a partial fulfillment of the requirements for a degree from Emory University, I hereby grant to Emory University and its agents the non-exclusive license to archive, make accessible, and display my thesis in whole or in part in all forms of media, now or hereafter now, including display on the World Wide Web. I understand that I may select some access restrictions as part of the online submission of this thesis. I retain all ownership rights to the copyright of the thesis. I also retain the right to use in future works (such as articles or books) all or part of this thesis.

Michael Sau April 8, 2022

Investigating the therapeutic role of EP2 antagonism in two-hit mouse model of Alzheimer's disease

By

Michael Sau

Thota Ganesh, PhD.
Adviser

Human Health

Thota Ganesh, PhD

Adviser

Amanda Freeman, PhD.

Committee Member

Megan Cole, PhD.

Committee Member

Kristen Frenzel PhD.

Committee Member

2022

Investigating the therapeutic role of EP2 antagonism in two-hit mouse model of Alzheimer's disease

By

Michael Sau

Thota Ganesh, PhD.
Adviser

An abstract of a thesis submitted to the Faculty of Emory College of Arts and Sciences of Emory University in partial fulfillment of the requirements of the degree of
Bachelor of Arts with Honors

Human Health

2022

Abstract

Investigating the therapeutic role of EP2 antagonism in two-hit mouse model of Alzheimer's disease
By Michael Sau

Alzheimer's disease (AD) is a neurodegenerative disorder, characterized by loss of neurons, the formation of pathological proteins like amyloid-beta (Aβ), and activation of glial cells in the brain leading to progressive cognitive decline and dementia. So far, there is no drug available to treat the underlying pathology of AD. In our laboratory, we have demonstrated that the prostaglandin E2 receptor (EP2) has a role in neuroinflammation in mouse models of neurodegeneration and small molecule EP2 inhibitors attenuate the robust inflammatory bursts following status epilepticus in rodents. The overall goal of this study is to further investigate the therapeutic efficacy of our EP2 antagonist in ameliorating AD pathology and inflammation. Here, we aim to use a two-hit model of Alzheimer's disease where transgenic 5xFAD mice are subjected to an external stimulus of lipopolysaccharide (LPS) to induce an additional level of inflammation in the AD brain. Subsequently, cohorts of mice will be treated with a potent and selective EP2 antagonist (TG11-77.HCl) added to the drinking water and their brains will be investigated for amyloid pathology and associated neuroinflammation by qRT-PCR as well as immunohistological staining and quantification. The results show that administration of LPS to 5xFAD mice results in a more robust neuroinflammation compared to non-LPS treated mice, which was similar to results that were found in previous studies in our laboratory. Furthermore, we demonstrate attenuation of neuroinflammation, gliosis and amyloid pathology by selective inhibition of the EP2 receptor with the TG11-77.HCl compound. This study strengthens the candidacy of the EP2 receptor as a therapeutic target for combating AD pathology.

Investigating the therapeutic role of EP2 antagonism in two-hit mouse model of Alzheimer's disease

By

Michael Sau

Thota Ganesh, PhD
Adviser

A thesis submitted to the Faculty of Emory College of Arts and Sciences
of Emory University in partial fulfillment
of the requirements of the degree of
Bachelor of Arts with Honors

Human Health

2022

Acknowledgements

I would like to thank Dr. Asheebo Rojas, and Dr. Avijit Banik, for support and guidance throughout the course of this project. I would also like to thank Dr. Kristen Frenzel, Dr. Amanda Freeman, and Dr. Megan Cole for serving on my Honors Thesis Committee. I would also like to thank Dr. Thota Ganesh for also serving on my committee and giving me the opportunity to perform my senior Honors Thesis in his lab. Finally, I would like to thank Dr. Raymond Dingledine for his never-ending support during my time in his lab. He provided me with a lab space and resources necessary for me to be able to succeed.

Table of Contents

Investigating the therapeutic role of EP2 antagonism in two-hit mouse model of Alzheimer's disease

Michael Sau

Department of Pharmacology, Emory University School of Medicine , Atlanta, GA 30322, USA

Key Words

Alzheimer's disease, inflammation, gliosis, pro-inflammatory cytokines, chemokines, two-hit 5xFAD, EP2, lipopolysaccharide, TG11-77.HCl

Abbreviations

Alzheimer's disease (AD), familial Alzheimer's disease (FAD), beta-amyloid (Aβ), neurofibrillary tangles (NFTs), late onset Alzheimer's Disease (LOAD), early onset Alzheimer's Disease (EOAD), amyloid-precursor protein (APP), presenilin 1 and 2 (PSEN1 and PSEN2), prostaglandin E_2 receptor 2 (EP2), non-steroidal anti-inflammatory drugs (NSAIDs) central nervous system (CNS), cerebrospinal fluid (CSF), β-secretase 1 (BACE1), quantitative real-time polymerase chain reaction (qRT-PCR), prostaglandin (PGH2), prostaglandin EP2 (PGE2), protein kinase A (PKA), Nicotinamide adenine dinucleotide phosphate (NADPH) oxidase (NOX), Triggering receptors expressed on myeloid cells 2 (TREM2), miconazole (MCZ), Interleukin 1 beta (IL-1β), Interleukin 6 (IL-6), Interleukin 18 (IL-18), Tumor necrosis factor-α (TNF-α), TNF receptor 1 (TNFR 1), TNF receptor 2 (TNFR2), Interleukin 4 (IL-4), Chemokine (C-C motif) ligand 2 (CCL2), CCR2 (C-C Motif Chemokine Receptor 2), CCR5 (C-C Motif Chemokine Receptor 5), (Chemokine (C-C motif) ligand 3) CCL3, (Chemokine (C-C motif) ligand 4) CCL4, macrophage inflammatory protein 1a (MIP-1a), macrophage inflammatory protein 1-β (MIP1-β), Calcium-binding adaptor molecule 1 (Iba1), Cluster of differentiation 68 (CD68), Blood brain barrier integrity (BBB), glial fibrillary acidic protein (GFAP), calcium-binding protein (S100B), toll-like-receptor 4 (TL4), National Institutes of Health (NIH), Institutional Animal Care and Use Committee (IACUC), non-transgenic (nTg), beta-actin (β-actin), glyceraldehyde-3-phosphate (GAPDH), and hypoxanthine phosphoribosyl transferase 1 (HPRT1),phosphate buffered saline (PBS), antigen (Ag), Congo red (CR)

Introduction

Background

Alzheimer's disease (AD) is a worldwide public health issue, where over 6.2 million Americans aged 65 and older are diagnosed with Alzheimer's disease (*2021 Alzheimer's disease facts and figures*, 2021). With the ever-increasing number of AD patients, it is important to provide optimal treatment and care for those with AD as this disease is debilitating. With life expectancy in the US getting higher due in part to medical advances it is predicted that healthcare cost for AD patients will increase.

Alzheimer's disease is one of the most common neurodegenerative diseases that progressively causes memory impairment, cognitive decline, and speech problems (DeTure & Dickson, 2019). The disease is characterized by a loss of neurons, the formation of pathological proteins like amyloid β (Aβ) in extracellular space and intracellular neurofibrillary tangles (NFTs) composed of the tau protein, and neuroinflammation, including activation of non-neuronal cells known as glia in the disease brain (Azizi et al., 2015). In the aging human brain, there is a decrease in the amyloid β clearing mechanism and a decrease in memory function with progressing age as the excitatory synapses of neurons start decaying (Dal Pra et al., 2008). Amyloid β plaques are generated from the proteolysis of the amyloid precursor protein (APP) via β- and γ-secretase enzyme activities (Chow et al., 2010). Beta-site APP cleaving enzyme 1 (BACE1) is involved in the cleavage of APP, leaving carboxyterminal fragments-99 (CTF-99) (Chow et al., 2010) to be cleaved by a γ-secretase complex composed of glycoproteins Presenilin-1 (PSEN1) and Presenilin-2 (PSEN2), forming the Aβ peptides (O'Brien & Wong, 2011).

One of the most important risk factors for AD is age, with around 95 percent of late onset Alzheimer's Disease (LOAD) cases appearing after 65 years of age (Guerreiro & Bras, 2015).

There is, however, an increasing recognition of pathophysiological processes that may occur before patients present clinical symptoms of Alzheimer's disease (Tan et al., 2014). Those with early onset Alzheimer's Disease (EOAD) are classified as patients who are < 65 years of age (Dai et al., 2017). These patients account for around 5% of diagnosed Alzheimer's Disease patients (DeTure & Dickson, 2019). Genetic factors play a major role in these cases, with three notable genes that encode for proteins involved in amyloid precursor protein (APP) breakdown and amyloid-beta (Aβ) generation: the *APP* gene, the presenilin 1 (*PSEN1*) gene, and presenilin 2 gene (*PSEN2*) (Dai et al., 2017).

In patients with Alzheimer's disease, the neurofibrillary tangles contain tau proteins that are hyperphosphorylated in the brain compared to brains of people that do not have AD (Metaxas & Kempf, 2016). In healthy brains, the tau protein promotes and stabilizes microtubule assembly, playing a key role in cognitive processes (Alonso et al., 2018). Hyperphosphorylation of the tau protein, however, results in the aggregation of tau proteins, inhibiting microtubule assembly (Alonso et al., 2018), synaptic loss, and memory impairment in patients with AD (Metaxas & Kempf, 2016). A common pathology in AD is neuroinflammation, which is the brain's physiological immune response against harmful stimuli (Newcombe et al., 2018), and plays a key role in AD pathology. In the brain, there are several components in the immune response, including, but not limited to, changes in the structure and function of microglia and astrocytes, as well as changes in the levels of cytokines, chemokines (Tuppo & Arias, 2005), and other inflammatory mediators such as enzymes like cyclooxygenase-2 (COX-2). In AD animal models, cytokines and chemokines in general have been shown to be elevated compared to wildtype controls (Tuppo & Arias, 2005). In conjunction with the accumulation of Aβ and NFT pathologies, the elevated inflammatory mediators result in the persistent impairment of glial cells and a sustained immune

response (Heneka et al., 2015). Impairment of these glial cells can lead to a chronic activation of astrocytes and microglia, leading to the production of pro-inflammatory cytokines and chemokines, and ultimately, neuroinflammation. One question that remains in AD pathology is whether the expression level of the inflammatory mediators change prior to the buildup of Aβ and NFT in the brain or whether neuroinflammation is a secondary response to Aβ and NFT. The attenuation of these inflammatory mediators and biomarkers before clinical symptoms arise may be beneficial in understanding and developing treatments to slow the progression of AD.

Proinflammatory Mediators

Neuroinflammation is an important homeostatic feature following an injury and it involves the induction of proinflammatory and anti-inflammatory mediators. A key protein that is induced following an injury is COX-2. COX-2 is an inflammatory mediator that is a rate-limiting enzyme in the synthesis of five prostaglandins (PGD2, PGE2, PGF2, PGI2, and TXA2) (Ganesh, 2014). COX-2 expression in neurons rapidly increases in response to an injury (Simon, 1999). The prostaglandin PGE2 binds to receptors such as the prostaglandin E_2 receptor 2 (EP2), which helps to upregulate inflammation at sites of injury or illness (Ganesh, 2014). In the AD brain, elevated levels of COX-2 indicate a potential involvement in a cascade of events leading to neurodegeneration, as indicated by the Braak score (Wang et al., 2014).

The Braak score is a neuropathological staging of AD, based on the distribution of NFTs in AD pathology (Bancher et al., 1993). Stages I and II (Braak A) are the first stages in AD pathology, followed by stages III and IV, and stages V and VI (Bancher et al., 1993). COX-2 positive neurons are most abundant in the initial stages of AD, Braak A, decreasing with the severity of AD (Minghetti, 2004). As COX-2 has been detected in earlier stages of AD, Braak A,

these findings may indicate a potential therapeutic opportunity for pre-symptomatic stages of AD (Wang et al., 2014).

Though non-steroidal anti-inflammatory drugs (NSAIDs) generally inhibit COX-1 and COX-2 (Wyss-Coray, 2006), targeting and inhibiting the cyclooxygenases gene may be too broad for obtaining specific effects, resulting in issues outside of the brain, like cardiovascular side effects as was the case for Vioxx (Ganesh, 2014). As a key feature of inflammation is to induce a beneficial response, broad inhibition of inflammation via NSAIDs may be detrimental in neurodegenerative diseases like AD (Wyss-Coray, 2006) and should be avoided.

Targeting the specific downstream prostanoid receptors with selective modulators may offer an alternative to the broad effects of cyclooxygenases. For example, the use of anti-inflammatory drugs to target the EP2 receptor in microglial cells and reduce inflammation has been seen as a potential avenue for therapeutic approaches (Ganesh, 2014). While a COX-2 inhibitor would affect multiple prostanoid receptor signaling cascades, the use of an EP2 receptor may avoid the detrimental side effects of COX-2 inhibition. In the COX-2 signaling cascade, the intermediate prostaglandin (PGH2) is converted into prostaglandin ligands that activate G-protein coupled receptors (Ganesh, 2014). The activation of the prostaglandin E2 (PGE_2) receptor, EP2, which is Gαs-coupled receptor, stimulates adenylate cyclase, and increases cellular cAMP (Rojas et al., 2020). This cAMP can either activate protein kinase A (PKA), and/or the exchange protein activated by cAMP-1 (Epac)-signaling (Ganesh, 2014). EP2 activation results in elevated expressions of IL-6, IL-1β, and decreasing expression of TNFα and CCL2 (Rojas et al., 2020). It is currently unknown as to exact the mechanisms by which EP2 regulates inflammation, but studies have shown that loss of EP2 reduces the amount of Aβ peptides in the AD brain, and inhibition of EP2 with selective EP2 antagonists like TG6-10-1 or TG11-77.HCl results in less inflammation

following an injury (Ganesh, 2014). Therefore, utilizing a selective antagonist to block EP2 may be beneficial as a therapeutic approach to combating AD.

Figure 1 demonstrates the interaction between the NOX2 subunits. Nicotinamide adenine dinucleotide phosphate (NADPH) oxidase (NOX) is an oxidant-producing enzyme found in neutrophils (Gong et al., 2020). NOX produces reactive oxygen species (ROS), inducing oxidative stress, which contributes to Amyloid-β pathology and AD pathogenesis (Gong et al., 2020). NOX2 ($gp91^{phox}$) is one of the enzymes of the NOX family, and generates superoxide as its product (Ma et al., 2017). While NOX2 is expressed in various tissues of the body, it is most abundant in microglia as it is involved in the inflammatory response after injury (Ma et al., 2017). During activation, a phosphorylated $p47^{phox}$ interacts with $p22^{phox}$ to form the NOX2 complex (Ma et al., 2017). Considering this, $p47^{phox}$ plays a key role in organizing phagocyte oxidase subunits for NOX2 activation (Gong et al., 2020).

In the AD model, $p47^{phox}$ deficiency has been shown to significantly improve cognitive impairment, and attenuate tau pathology (Gong et al., 2020). Understanding the role of NOX2 in AD and $p47^{phox}$ may provide a new strategy of treatment for AD (Fig. 1). Inducible nitric oxide synthase (iNOS) is a family of enzymes that generate nitric oxide (NO), and other NO-derived reactive nitrogen species (Nathan et al., 2005). In AD, iNOS was identified in the AD lesions, indicating immunoreactivity in neurons and astrocytes in the brain (Nathan et al., 2005). An accumulation of iNOS may induce issues such as DNA oxidative damage, and neuronal disruption (Medeiros et al., 2007), whereas a deficiency in iNOS inhibited accumulation of Amyloid-β plaques (Nathan et al., 2005), indicating that an inhibition of iNOS could be a potential therapeutic option in AD. Currently, the antifungal drug, miconazole (MCZ), has been shown to attenuate cognitive impairment, suppression of iNOS and COX-2 expression, and reduced cytokine levels

in the brain (Yeo et al., 2020). The utilization of MCZ to target iNOS may be seen as a potential therapeutic strategy in AD pathogenesis.

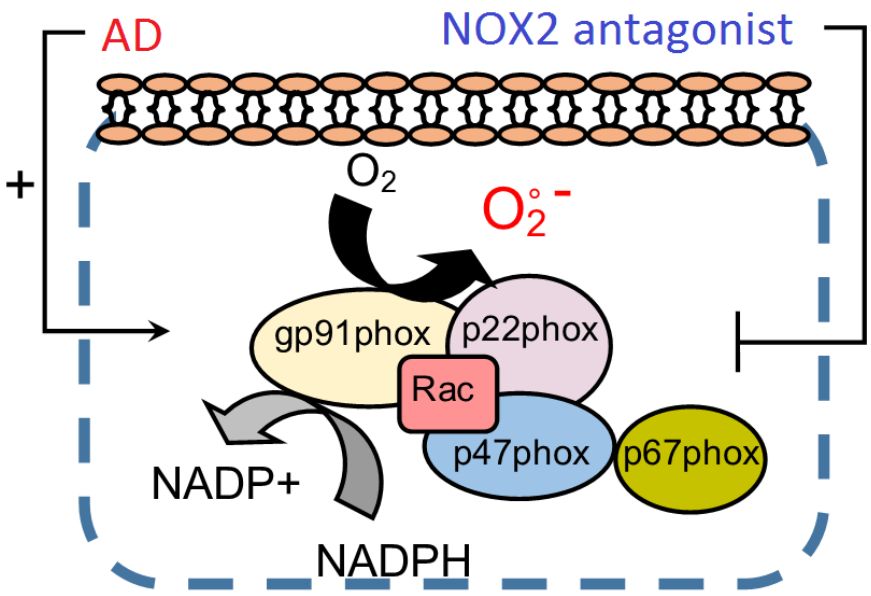

Figure 1: Interaction of the NOX2 subunits (gp91-*phox, and p22-phox)*. The NOX complex forms several systolic subunits (p47-*phox*, p67-*phox)*, as well as the G-protein *Rac*, which is involved in the activation of NOX. The activated NOX generates superoxide ion. The NADPH acts as a substrate for NOX, which produces ROS, inducing oxidative stress, contributing to Amyloid-β pathology and AD pathogenesis. The NOX2 antagonist may function to inhibit NOX in several ways: 1) inhibiting p47-*phox* interactions; 2) inhibiting phosphorylation via PKC to prevent NOX activation; 3) acting on gp91-*phox* to prevent NOX activation and assembly; 4) an unknown mechanism.

Triggering receptors expressed on myeloid cells 2 (TREM2) are expressed by microglia in the brain (Gratuze et al., 2018). TREM2 is essential in the maintenance of microglial metabolic fitness during stress events, namely, the microglial response to Amyloid-β pathology (Ulland & Colonna, 2018). As such, studies have demonstrated that a loss of TREM2 in microglia inhibited phagocytosis of apoptotic neurons and debris (Takahashi et al., 2005), indicating that TREM2 functions to increase the rate of phagocytosis. TREM2 has been found to increase Late onset Alzheimer's disease risk by 2-4-fold (Gratuze et al., 2018). Measuring TREM2 expression may

help in understanding LOAD neuropathology and bring insight into the effects of gliosis in neurodegeneration. An anti-human TREM2 monoclonal antibody, AL002, has shown promising results as it decreased the microglial inflammatory response, and was well tolerated in a phase I clinical trial (Wang et al., 2020).

Cytokines in AD

Cytokines are small, nonstructural proteins that include interleukins, interferons, and tumor necrosis factors (Monastero & Pentyala, 2017). These cytokines play a key role in inflammatory processes in AD pathogenesis (Rubio-Perez & Morillas-Ruiz, 2012).

Interleukin 1 beta (IL-1β) is a proinflammatory cytokine involved in the upregulation of APP through the activation of protein kinase C and increased γ-secretase activity (Kinney et al., 2018). In addition, the overexpression of IL-1β exacerbates tau phosphorylation and tangle formation, which impacts cognitive functions like learning and memory (Wang et al., 2015). There are, however, many unknowns in the underlying mechanisms of IL-1β function. Studies have shown a beneficial role of IL-1β, where the overexpression of IL-1β may reduce Amyloid-β-related pathology through microglia-dependent plaque degradation (Wang et al., 2015). On the other hand, other studies have shown an increase in Amyloid-β burden and plaque deposition as microglial Amyloid-β clearance functions are impaired in response to IL-1β production (Kinney et al., 2018). More detailed studies are needed to get a better understanding of the role of IL-1β in AD pathology.

Interleukin 6 (IL-6) is a pro-inflammatory cytokine involved in the homeostasis of neuronal tissue, wherein the removal of the signaling pathway reduces microglial activation, but overproduction of IL-6 leads to chronic neuroinflammation and neurodegeneration (Kinney et al., 2018). Elevated levels of IL-6 have been detected in the brain, cerebrospinal fluid, and around

amyloid plaques in AD, indicating that IL-6 may be involved in AD related neuroinflammation (Wang et al., 2015). In addition, IL-6 has been shown to contribute to NFT formation (Wang et al., 2015) via hyperphosphorylation of tau proteins (Kinney et al., 2018). Through this, there may be a potential dual linkage of Aβ burden, tau hyperphosphorylation, and neuroinflammation in AD where neuroinflammation in AD may increase amyloid burden, as well as tau hyperphosphorylation (Kinney et al., 2018).

Interleukin 18 (IL-18) is a proinflammatory cytokine that is produced through activated microglia, astrocytes, ependymal cells, and neurons in the central nervous system (CNS), (Wang et al., 2015). IL-18 may contribute to apoptosis (Wang et al., 2015), and is involved in aging and neurodegeneration, increasing the risk of IL-18 levels and AD progression (Su et al., 2016). In AD, amyloid-β may be involved in the upregulation of IL-18, and consequently, tau phosphorylation, which indicates that IL-18 may contribute with the neuroinflammatory response (Ojala et al., 2009).

Tumor necrosis factor-α (TNF-α) is a proinflammatory cytokine that plays a central role in the initiation and regulation of the cytokine cascade (Kinney et al., 2018). TNF-α binds to the TNF receptor 1 (TNFR 1) and TNF receptor 2 (TNFR2) receptors, allowing for Amyloid β-induced neuronal apoptosis (Kinney et al., 2018). They are also involved in processes like cell proliferation and cell migration (Wang et al., 2015). It has been shown in APP transgenic mice that the deletion of the TNFR 1 gene reduced plaque deposition by down-regulating BACE1 activity (Wang et al., 2015), decreasing microglial activation, and improving cognitive tasks (Kinney et al., 2018). In AD, TREM2 plays a role in neurodegeneration through the regulation of phagocytic processes, myeloid cell survival and proliferation, as well as regulation of inflammation (Kinney et al., 2018).

Overall, a TREM2 deficiency shows a decreased capacity to clear amyloid-β, as well as tau pathology.

Interleukin 4 (IL-4) is an anti-inflammatory cytokine that can suppress proinflammatory cytokine production and action (Rubio-Perez & Morillas-Ruiz, 2012). These cytokine-cytkoine interactions play a crucial role in AD neuroinflammation as a dysregulation of the proinflammatory and anti-inflammatory cytokines may induce cytotoxicity (Rubio-Perez & Morillas-Ruiz, 2012). Cytokines like IL-4 may play a role in neutralizing neuroinflammatory processes in the brain (Su et al., 2016). It has been shown that IL-4 induces microglial clearance of Amyloid β and alleviates cognitive impairment in AD animal models (Su et al., 2016).

Chemokines in AD

Chemokines are a subset of proteins that are chemotactic, and they play a role in regulating immune cell migration to sites of inflammation (Zuena et al., 2019). Chemokines are involved in neuroinflammatory and neurodegenerative processes (Martin & Delarasse, 2018) through the binding of chemokine receptors that are classic G-protein-coupled receptors, including the downregulation of acetylcholine levels (Zuena et al., 2019). In addition, chemokines are involved in neuroinflammation by promoting glial cell activation in the plasma, CSF, and brain tissue of patients with AD (Zuena et al., 2019). Chemokines have a crucial role in the CNS, including brain development, as well as neuroinflammation (Martin & Delarasse, 2018). In AD, chemokines play a role in the development of amyloid β plaques by producing and regulating amyloid β peptides, and the phosphorylation of Tau, contributing to neurofibrillary tangles (Martin & Delarasse, 2018).

Chemokine (C-C motif) ligand 2 (CCL2), also known as monocyte chemoattractant protein 1 (MCP-1), is produced by microglia and astrocytes in pathological conditions (Martin & Delarasse, 2018). CCL2 is one of many chemokines that activate the CCR2 (C-C Motif

Chemokine Receptor 2) (Martin & Delarasse, 2018). It has been shown through clinical data of AD patients that CCL2 levels increase in CSF and in plasma, correlating to both the progression of the disease, as well as cognitive decline (Zuena et al., 2019). Essentially, CCL2 is involved in the recruitment of peripheral inflammatory monocytes expressing CCR2 (Martin & Delarasse, 2018). There is, however, evidence that a lack of CCL2 may accelerate the disease progression as a CCR2 deficiency accelerates memory deficits and disease progression through the increase of amyloid-β levels in the brain, because of impaired macrophage recruitment, microglial accumulation, and amyloid-β clearance (Zuena et al., 2019). Another study demonstrated this with the mouse model Tg2576, where a lack of CCR2 increased amyloid-β load and mortality (Martin & Delarasse, 2018). The CCR5 (C-C Motif Chemokine Receptor 5) receptor binds chemokine (Chemokine (C-C motif) ligand 3) CCL3, and Chemokine (C-C motif) ligand 4 (CCL4) ligands. CCL3, also known as macrophage inflammatory protein 1a (MIP-1a), plays a role in AD pathogenesis through the accumulation of activated glial cells, resulting in inflammation and cognitive failure via Amyloid-β load (Martin & Delarasse, 2018). In an AD model comparing Wild-Type C57BL/6, MIP-1α−/−, and CCR5−/− , it has been shown that either a CCL3 or CCR5-deficiency resulted in decreased cognitive impairments and inflammation through a decrease in amyloid-β load (Passos et al., 2009). The activation of CCL3/CCR5 signaling pathways results in an increased accumulation of glial cells, resulting in an inflammatory response and cognitive failure (Azizi et al., 2014). CCL4, or macrophage inflammatory protein 1-β (MIP1-β), plays a potential role in AD pathogenesis as CCL4 and the CCR5 receptor are expressed in reactive astrocytes in patients with AD (Zhu et al., 2014). Though the role of CCL4 is unclear, an overexpression of CCL4 mRNA in APP/PS1 mouse models have shown an age-related increase in amyloid-β load (Vérité et al., 2018).

Gliosis in AD

Glial cells are located within the CNS and respond quickly to brain injuries to restore normal brain physiology (Bronzuoli et al., 2016). In AD, cognitive impairments and memory loss are associated with amyloid–β accumulation, subsequently activating glial cells to remove the aggregate amyloid–β plaques (Kim et al., 2018). In essence, gliosis (glial cell activation) is a protective mechanism in response to a stimulus, but prolonged activation may cause detrimental effects (Bronzuoli et al., 2016). Microglia and astrocytes are the two most studied types of glial cells that are further discussed below.

Microglia help to form the brain's innate immune response and promote homeostasis in the brain (Neumann et al., 2009). Microglia also play a potential neuroprotective role in AD. Activated microglia reduce amyloid–β accumulation via phagocytosis, clearance, and degradation (Bronzuoli et al., 2016). Phagocytic clearance after injury plays a role in triggering repair. The activated microglia are recruited to the injured areas of the brain and stimulates an inflammatory response. In the Alzheimer's disease mouse model, microglia phagocytize amyloid–β plaques, dead cell debris or other neurotoxins. Activated microglia release cytokines and chemokines to begin repair and create an environment that promotes regeneration (Neumann et al., 2009). In AD, a prolonged activation of microglia results in the release of excess chemokines leading to chronic neuronal damage and resulting in suppression or over activation of other glial cells in a feedback mechanism (Kim et al., 2018).

There are several markers that can be used to visibly identify microglia in tissue such as cluster of differentiation molecule 11b (CD11b) and ionized calcium-binding adaptor molecule 1 (Iba1). Iba1 is a cytoplasmic protein expressed in the brain that increases upon microglial activation (Hopperton et al., 2018). Iba1 plays an important role in the formation of actin bundles,

allowing for microglial migration and phagocytosis (Franco-Bocanegra et al., 2019). In addition, CD11b is a marker that helps in the recognition and phagocytosis of antigens like amyloid-β (Hopperton et al., 2018). CD11b is expressed in both resting and activated microglia (Hopperton et al., 2018). Cluster of differentiation 68 (CD68) is another marker for microglial expression. CD68 labels lysosomes, making it a marker for activated phagocytic microglia (Hopperton et al., 2018).

Astrocytes are important in the CNS as they are involved in important mechanisms including maintenance of homeostatic balance, inflammation, and maintenance of the blood brain barrier integrity (BBB) (González-Reyes et al., 2017). Astrocytes are an essential part of the inflammatory response of the CNS involved in the production, degradation, and removal of amyloid-β (González-Reyes et al., 2017). Reactive astrogliosis (astrocyte activation and swelling) in AD can be initiated via damaged neurons, or from amyloid-β aggregation (Verkhratsky et al., 2010). These activated astrocytes contribute to neuroinflammation in AD through the release of cytokines, and various proinflammatory factors (Verkhratsky et al., 2010).

Astrocytes express markers such as glial fibrillary acidic protein (GFAP) and calcium-binding protein (S100B). GFAP is an astrocytic cytoskeletal protein that serves as a marker for the activation and proliferation of astrocytes (Chatterjee et al., 2021). In AD, amyloid-β plaques are surrounded by astrocytes, displaying increased expression of GFAP (Kamphuis et al., 2014). S100B is a calcium-binding protein that acts as a pro-inflammatory cytokine (Cristóvão & Gomes, 2019). In AD, S100B secreted from astrocytes is postulated to regulate amyloid-β plaque formation and promote an inflammatory response in the brain (Cristóvão & Gomes, 2019).

Lipopolysaccharide and AD

Neuroinflammation is an important process in triggering the neurodegenerative process (Batista et al., 2019). Lipopolysaccharides (LPS) is a molecule present in the outer membrane of Gram-negative bacteria and activates various targets like the toll-like-receptor 4 (TL4) (Batista et al., 2019). LPS treatment causes central nervous system inflammation. LPS triggers CNS inflammation, which is characterized by interleukin-1β and tumor necrosis factor-α induction and release, microglial and astrocytic activation, and increase in APP (Sheng et al., 2003). LPS increases the number and size of microglia and astrocytes, and expression of several glial markers. These results are exacerbated in the presence of an APP mutation, where these individuals cause accelerated for deposits in the brain (Sheng et al., 2003). Lee et al., 2008 demonstrated an increase in immunoreactivity in the LPS injected cohort compared to that of the control group, particularly in the hippocampal area. In addition, LPS alone induced cognitive impairment in mice (Lee et al., 2008), making LPS an important tool in modeling neuroinflammation. Overall, LPS can be utilized in conjunction with a genetic AD model to replicate a "two-hit" AD model.

Rationale

The 5xFAD mouse in a B6SJL strain has demonstrated AD-related symptoms earlier than other animal models, indicating that this may be a beneficial mouse model to study for amyloid deposition and neurodegeneration starting at 2 months of age (Landel et al., 2014). The transgenic model used in this study express mutant human amyloid beta (A4) precursor protein 695 (APP) with the Swedish (K670N, M671L), Florida (I716V), and London (V717I) mutations along with two human familial Alzheimer's Disease (FAD) mutations on PSEN1(M146L and L286V) (Oblak et al., 2021). The Swedish double mutation (K670N/M671L) clusters near β-secretase sites and forms greater amounts of amyloid β deposition, while the London (V717I) and Florida (I716V) mutation increases the generation of amyloid β (Oakley et al., 2006). The two FAD mutation on

PSEN1 gene are found on chromosome 14 and regulates γ-secretase activity to release Aβ peptides (Weggen & Beher, 2012). These 5xFAD mice display amyloid deposition, gliosis, and progressive neuronal loss accompanied by cognitive and motor deficiencies, which models features like AD and its disease progression (Oblak et al., 2021). One limitation, however, is that 5xFAD mice do not display NFTs, indicating that there may be differences in this mouse model and human AD (Oakley et al., 2006).

This study aims to highlight the potential therapeutic opportunity of EP2 receptor inhibition. Previous work done on a 5xFAD C57BL6/SJL mice background demonstrated a reduction in proinflammatory mediators and glial markers by an EP2 antagonist for a two-hit cohort of females (Banik et al., 2021). In addition, the EP2 inhibitor demonstrated a reduction in select proinflammation mediators and glial markers in a two-hit female model induced with LPS (Banik et al., 2021). In this study, we further characterize the efficacy of the EP2 antagonist in a two-hit rodent AD model using a different mice background strain. In this particulat 5xFAD model, amyloid deposition and gliosis begins at 2 months, progressively increasing the disease burden (Oakley et al., 2006).

Hypothesis

If there is an oral dosing of a selective and potent EP2 antagonist (TG11-77.HCl), then the EP2 antagonist should significantly reduce the amyloid burden and associated neuroinflammation in the 5xFAD brains. Furthermore, we investigated whether a robust LPS-induced inflammation can be ameliorated with the EP2 antagonist, comparing the one- and two-hit mouse models.

Materials and Methods

Animals

All experiments involving animals conformed to the guidelines of the National Institutes of Health (NIH) and the Emory University Institutional Animal Care and Use Committee (IACUC). Male and Female 5xFAD mice and non-transgenic (nTg) controls in the B6SJL background were used in this study. The mice are B6SJL Tg6799 mice bought from the Jackson Laboratories (Bar Harbor, ME) (JAX034848).

Study Design

This study aims to quantify gene expression, amyloid-β, and glial markers (mainly GFAP and Iba1) of 5-month-old 5xFAD mice in a one-and two-hit AD model. Cohorts of mice were administered LPS to mimic peripheral inflammation. The administration of LPS to the 5xFAD mice is the two-hit model compared to the single hit (genetic) expressing only Alzheimer's pathology. The cohorts of mice were comprised of both sexes of 5xFAD (one-hit - environmental) and their non-transgenic (nTg) littermates administered LPS (1mg/kg/week, intraperitoneally) (Sigma-Aldrich, St. Louis, MO) (two-hit - genetic and environmental) to induce additional brain inflammation (Fig. 2). An EP2 antagonist created in our laboratory (Amaradhi et al., 2020), or vehicle was given to mice in their drinking water bottles *ad libitum*. The mice were treated with either the EP2 antagonist, TG11-77.HCl (100 mg/kg/day), or its vehicle (drinking water without TG11-77.HCl adjusted to pH 3.5) via their drinking water (pH 3.5) for 12 weeks starting at 8 weeks of age. The mice are separated into 8 groups of 12 mice: male nTg and 5xFAD treated with an EP2 antagonist, male nTg and 5xFAD treated with only the vehicle for the EP2 antagonist, Female nTg and 5xFAD treated with EP2 antagonist, female nTg and 5xFAD treated with only the vehicle for the EP2 antagonist (Fig. 2). At the end of the experiments the mice were euthanized by overexposure to isoflurane, decapitated and tissues were collected for further analysis.

The neocortex and hippocampus were rapidly dissected from one-half brain and stored at -80°C until used to make cDNA, and measure mRNA levels of inflammatory mediators, cytokines, chemokines, and glial markers. The other half of the brain was fixed in 4% paraformaldehyde overnight at 4°C. The fixed half brains were then transferred to 30% sucrose (Sigma-Aldrich, St. Louis, MO) for at least 48 hours (until they sank), moved to phosphate buffered saline (PBS) (Sigma-Aldrich), and stored at 4°C until they were sectioned for immunohistochemical analysis.

RNA Extraction

Frozen neocortex tissues were homogenized on ice using a sonicator in 1 mL of RNA lysis buffer from the Quick-RNA MiniPrep Kit (Zymo Research, Irvine, CA) for 30 seconds. The homogenized tissue samples were then centrifuged at room temperature at 500g for 1 minute. The homogenate (700 µl of) was placed in a RNAse-free tube used for RNA extraction. An equal volume of 100% ethanol was added to the tube. The samples were centrifuged for 1 minute at 10,000 RPM. Using the Quick-RNA MiniPrep Kit (Zymo Research, Irvine, CA), the samples were washed with 400 µl of the wash buffer I and centrifuged for 1 minute at 10,000 RPM. To get rid of genomic DNA, 5µL of DNAse I + 75 µL of DNA Digestion Buffer was added to each cartridge (Zymo Research, Irvine, CA) and allowed to incubate at room temperature for 15 minutes. The RNA Prep Buffer (400 µl) was added to the samples, and they were centrifuged for 1 minute at 10,000 RPM. This step was repeated once. The samples were centrifuged for 1 minute at 10,000 RPM to get rid of the prep buffer in the cartridge and the samples were washed with the wash buffer. RNA was eluted with 50 µL of RNase-free water added to each cartridge. The samples were centrifuged at 10,000 RPM for 1 minute the the eluted RNA was stored frozen at -20°C until further use. The concentration of each sample was measured using an Epoch Microplate Spectrophotometer (BioTek, Winooski, VT).

cDNA Synthesis

RNA samples were converted into cDNA using the qScript cDNA SuperMix (Quanta Biosciences, Gaithersburg, MD) according to the manufacturer's protocol. Briefly, RNA (4 µg), RNase sterile water, and qScript cDNA SuperMix were added to Eppendorf tubes at a total volume of 60 µL. PCR (add the PCR protocol here) was performed to make cDNA. The cDNA samples were stored at -20°C.

Quantitative real-time polymerase chain reaction (qRT-PCR)

The reaction mixture of the qRT-PCR sample included SYBR Green Supermix (10 µL) (Quanta Biosciences, Gaithersburg, MD), a forward and reverse primer mix (0.5 µL each) of 10 µM, RNase free water (1 µL), and target cDNA (8 µL). Each sample was run in duplicates, with cycling conditions in the CFX96 Touch Real-Time PCR Detection System (Bio-Rad, Hercules, CA) were as follows: 95°C for 2 minutes, 40 cycles of 95°C for 15 seconds, and 60°C for 1 minute. Melting-curve analysis was used to verify the single species PCR product.

Three housekeeping genes, beta-actin (β-actin), glyceraldehyde-3-phosphate (GAPDH), and hypoxanthine phosphoribosyl transferase 1 (HPRT1) were used as internal controls. mRNA expression was measured for six pro-inflammatory receptors and enzymes [cyclooxygenase-2 (COX2), prostaglandin E2 receptor (EP2), p47phox, gp91phox, inducible nitric oxide synthase (iNOS), and triggering receptor expressed on myeloid cells 2 (TREM2)], eight cytokines and chemokines [interleukin-4 (IL-4), interleukin-6 (IL-6), interleukin-18 (IL-18), C–C motif chemokine ligands 2 (CCL2), C–C motif chemokine ligands 3 (CCL3), C–C motif chemokine ligands 4 (CCL4), tumor necrosis factor alpha (TNF), interleukin 1-beta (IL1β)], five glial markers [ionized calcium binding adaptor molecule (Iba1), glial fibrillary acidic protein (GFAP), Cluster of differentiation 11b (CD11b) and S100 calcium-binding protein B (S100B), and Cluster of

Differentiation 68 (CD68)]. The primer sequences used to quantify these genes of interest by qRT-PCR are listed in Table 4.

For qRT-PCR analysis, cycle threshold (CT) values for each gene of interest were normalized to the respective geometric means of CT values from all 3 housekeeping genes. The fold changes in the treatment groups were measured using the $2^{-\Delta\Delta Ct}$ method by calculating relative expression from the respective control groups (Livak & Schmittgen, 2001). The fold changes were used for statistical analysis between groups.

Neuroinflammation was determined by measuring the mRNA fold changes for selected gens of interests (GOI) that are known to be induced in the AD brain by qRT-PCR. The mRNA fold change for all genes of interest in the 5xFAD mice were compared to the mRNA fold change of the same gene in the respective nTg groups. In addition, we investigated whether EP2 antagonism can suppress chronic neuroinflammation in a two-hit model of 5xFAD (with LPS administration) in the brain by analyzing mRNA expression of selected genes.

Tissue sectioning

Coronal sections (30 µm) were cut using a cryostat (Leica, Wetzlar, Germany) and placed in a cryoprotectant media (450 µL PBS + 300 µL ethylene glycol + 250 µL glycerol) in a 24-well plate and stored at -20°C until further use.

Free Floating GFAP Stain

Sections were taken out of the freezing media and washed 3 times for 10 minutes each with phosphate buffered saline (PBS). Sections were then placed in sodium citrate buffered solution (Agilent, Santa Clara, Ca) for antigen (Ag) retrieval for 20 minutes at 98 ºC and then cooled at room temperature. To block nonspecific binding, 400 µL of blocking solution (100 µL 3% Triton + 50 µL Goat-serum + 850 µL PBS/mL)was added to the wells with the sections in 12-well plates.

The sections were blocked for 2 hours at room temperature. The sections were then incubated with the primary antibody [rabbit polyclonal to GFAP (Abcam, ab16997, 1:500 dilution)] diluted in a solution consisting of: 900 µL PBS + 100 µL 3% Triton + 20 µL Goat-serum and incubated at 4°C overnight. The following day, sections were washed 3 times for 10 minutes in PBS and subsequently incubated with a fluorescent conjugated secondary antibody diluted in the same solution as the primary antibody [Alexa Fluor goat anti-rabbit 488] (Thermofisher, Waltham, MA, A11008, 1:1000 dilution) and incubated for 2 hours at room temperature. The sections were washed 3 times for 5 minutes in PBS, mounted onto slides, dried and cover slipped with Fluoro-gel mounting media (Electron Microscopy Sciences, Hillsboro, OR).

Congo red staining

Congo red (CR) is a stain that is used to detect amyloid deposits in brain tissue (Wilcock et al., 2006). The CR dye interacts with the amyloid-β species and can be used in the development of detection for AD (Wu et al., 2012). Essentially, CR detects compacted amyloid in a beta-sheet secondary structure and labels amyloid aggregates (Wilcock et al., 2006).

Brain sections were selected for staining and measured for average plaque count of four sections per mouse. Sections were mounted on slides and left to dry. An activator solution (1% NaOH) was added to the preincubation solution "A" (80% ethanol + 2.5% NaCl), and the slides were placed in solution A for 25 minutes. An activator solution (1% NaOH) was added to Congo red staining solution "B" (80% ethanolic NaCl + 0.2% Congo red) and the slides were placed in solution "B" for 40 minutes. The slides were washed with PBS for 10 minutes and were hydrated with 80% ethanol for 1 minutes followed by 50% ethanol for 1 minute to remove excess stain. After washing the slides with PBS, the sections were coverslipped under DAPI (Vector Laboratories, Burlingame, CA) mounting media. Images were taken using the AxioObserver A1

fluorescence microscope (Zeiss, Dublin, CA) with the AxioVision AC 4.9.1 software (Zeiss, Dublin, CA).

Image quantification

Congo red, visualized by red fluorescence was analyzed using the ImageJ software (NIH Image, Bethesda, MD). The particle size, percent area covered by fluorescence, and total number of particles were quantified and compared between treatment groups. Each TIFF image was converted into an 8-bit image, thresholded, and an area of interest was selected. Images were then analyzed via the "Analyze particles" feature. Four sections were used per mouse, and the mean ± standard error was calculated for particle size, percent area covered by fluorescence, and total number of particles for each of the cohorts.

In addition, GFAP positive sections, visualized by a green, fluorescent signal were manually counted via the DotDot Goose software (American Museum of Natural History, New York, NY). Similarly, four sections were used per mouse, and the mean ± standard error were calculated for the number of astrocytes present for each cohort.

Statistical analysis

Data were statistically analyzed using GraphPad Prism version 9.0.0 (GraphPad, San Diego, CA). To determine the effect of LPS on mRNA expression, a one-way ANOVA with Dunnett's multiple comparisons test was used comparing the one-hit vehicle treated group to the two-hit vehicle treated group, and the one-hit TG11-77HCl treated group to the two-hit TG11-77HCl treated group. For group analysis, a paired t-test was applied between the one-hit vehicle treatment and the one-hit TG11-77 treatment, as well as the two-hit vehicle treatment and the two-hit TG11-77 treatment. In immunohistochemical quantification, an unpaired student's t test with multiple comparisons using two stage step-up (Benjamini, Krieger, and Yekutieli) with FDR (Q) = 5% was

used. The data are represented as Mean $\pm$ SEM for each group. The percent change in the expression of all markers in qRT-PCR is calculated by the formula: $\left(\left(\frac{Mean\ 2}{Mean\ 1}\right) - 1\right) * 100$ in the single-hit-environmental model and $\left(\left(\frac{Mean\ 2-1}{Mean\ 1-1}\right) - 1\right) * 100$ in the two-hit model, where Mean 1 represents the vehicle treated group and Mean 2 represents TG11-77. HCl treated group. The percent change in the immunohistological quantification was calculated by the formula: $\left(\frac{mean\ difference}{mean}\right) * 100$.

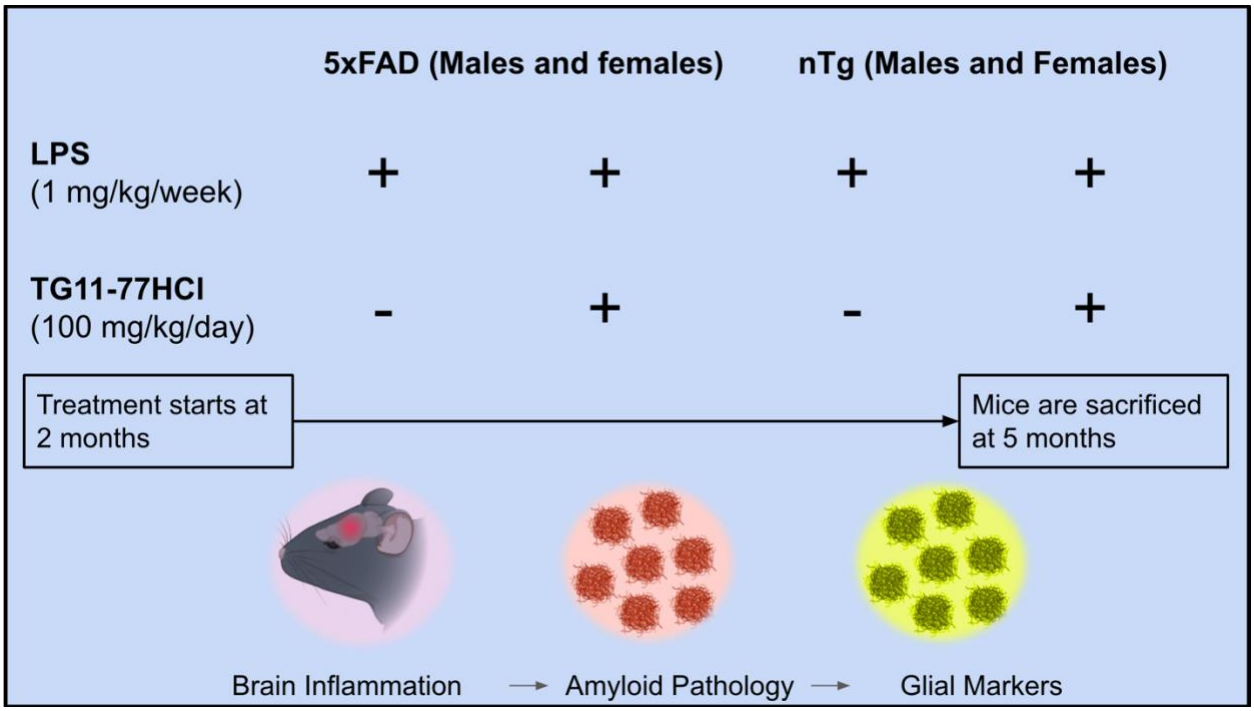

Figure 2. Experimental paradigm. Male and Female 5xFAD mice and non-transgenic (nTg) controls in the B6SJL background were used in this study to measure inflammation in the brain, Aβ pathology, and glial markers.

Results

Experiments were performed to investigate the effects of EP2 inhibition in a rodent model of Alzheimer's disease.

Expression of Proinflammatory Mediators

The levels of proinflammatory mediators gp91phox (One-Way ANOVA, p <.0001) and TREM 2 (One-Way ANOVA, p <.0001) were significantly upregulated in 5xFAD male mice (Fig. 3D, F and Table 1c), but iNOS levels were downregulated in one-hit male mice (One-Way ANOVA, p = .0183) treated with TG11-77.HCl (Fig. 3E and Table 1c). Similarly, there was an upregulation of proinflammatory mediators p47phox (One-Way ANOVA, p = .0455), gp91phox (One-Way ANOVA, p = .0022)and TREM2 (One-Way ANOVA, p <.0001) in 5xFAD female mice (Fig. 4C, D, F and Table 1d). The two-hit 5xFAD model displayed a more robust neuroinflammation as determined by the change in mRNA of inflammatory mediators compared to the one-hit model in both males and females (Fig. 3, 4 and Tables 1a, 1b). There was no significant decrease in proinflammatory mediators with an EP2 antagonist, TG11-77.HCl, for either the one-(paired t-test, p = .58) or two-hit 5xFAD (paired t-test, p = .053) male mouse model (Fig. 5B, D and Table 1e) nor a significant decrease by TG11-77.HCl for either one (paired t-test, p = .17) or two-hit 5xFAD (paired t-test, p = .38) female mouse (Fig. 5A, C and Table 1e).

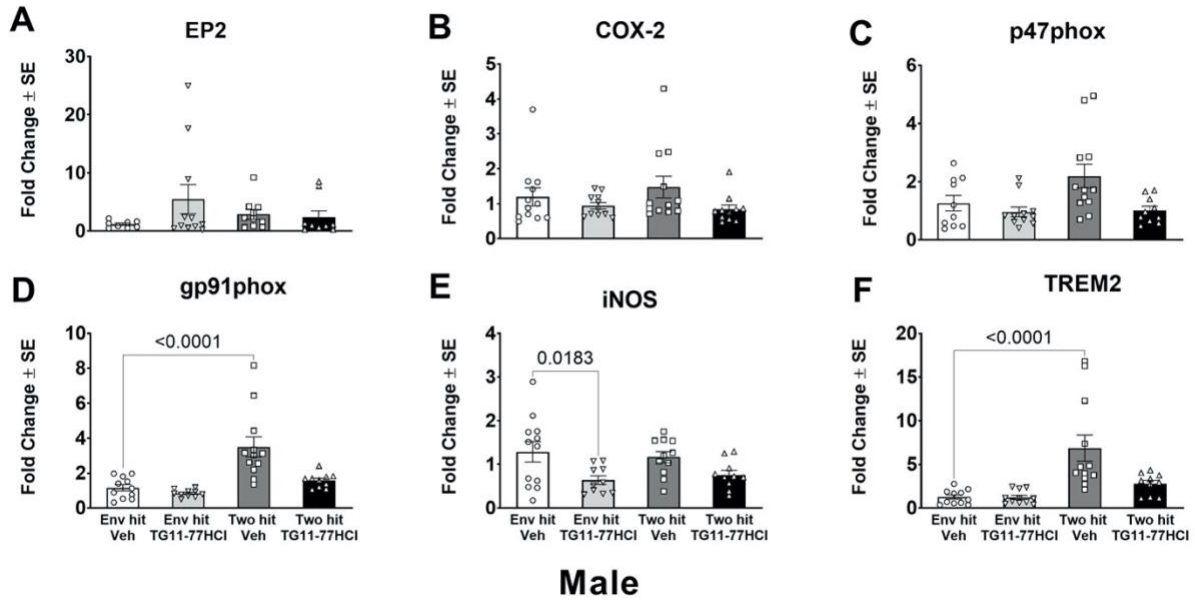

Figure 3. mRNA fold change of proinflammatory mediators (Males). *$p < 0.5$; **$p < 0.01$; ***$p < 0.001$; ****$p < .0001$ One-way ANOVA, Dunnett's multiple comparison test. Each symbol represents the mRNA fold change of an individual mouse. The bar graph represents the average of the groups. The bold horizontal bar is the mean, and the vertical bars are the standard error of the mean. Env hit is the environmental hit (single hit); two hit is the environmental hit with LPS administration; veh is the vehicle for TG11-77.HCl.

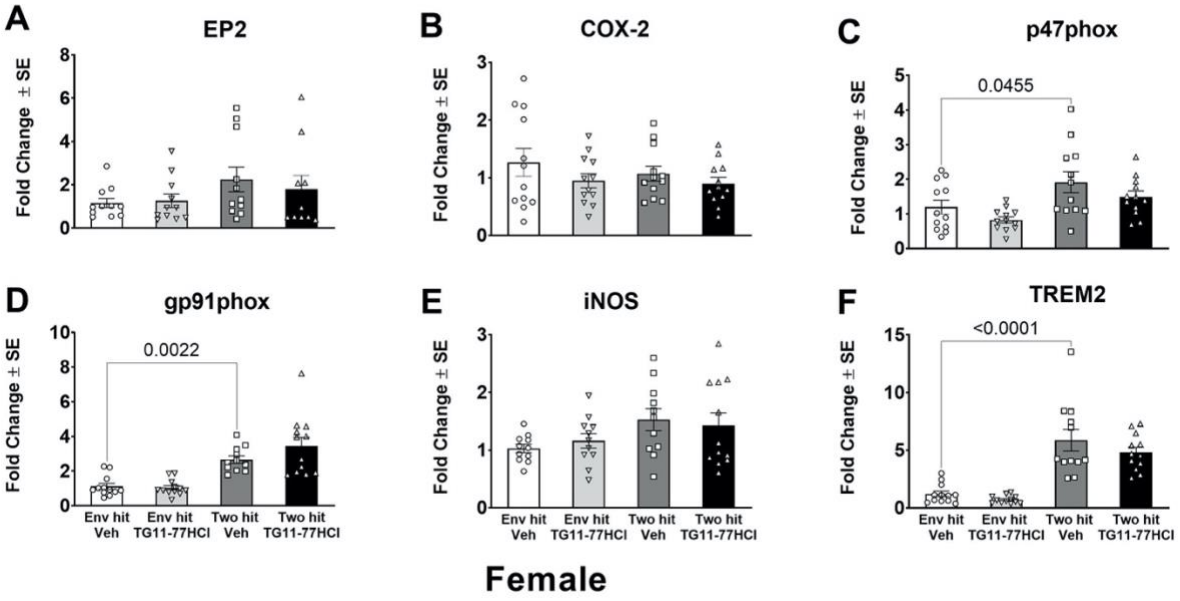

Figure 4. mRNA Fold Change of Proinflammatory Mediators (Females). (*$p < 0.5$; **$p < 0.01$; ***$p < 0.001$; ****$p < .0001$ One-way ANOVA, Dunnett's multiple comparison test). Each symbol represents the mRNA fold change of an individual mouse. The bar graph represents the average of the groups. The bold horizontal bar is the mean, and the vertical bars are the standard error of the mean. Env hit is the environmental hit (single hit); two hit is the environmental hit with LPS administration; veh is the vehicle for TG11-77.HCl.

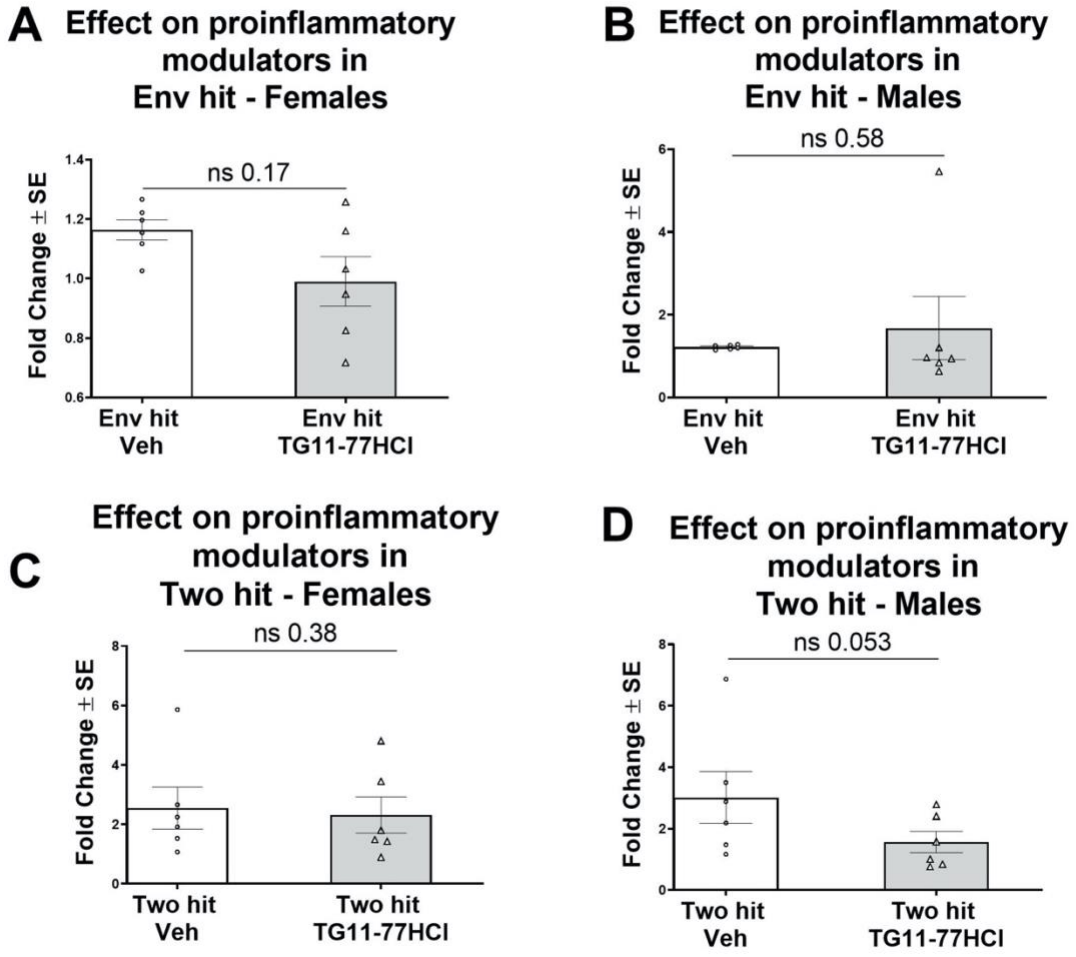

Figure 5. mRNA Fold Change Between All Proinflammatory Mediators Among Groups. (*p < 0.5; **p < 0.01; ***p < 0.001; paired t test). Each symbol represents the individual genes. The bar graph represents the average mRNA fold change for all genes in the group. Env hit is the environmental hit (single hit); two hit is the environmental hit with LPS administration; veh is the vehicle for TG11-77.HCl.

Upregulation of Select Cytokines and Chemokines

Some of the cytokines and chemokines were upregulated in both 5xFAD males (IL-6 (One-Way ANOVA, p = .0137), CCL3 (One-Way ANOVA, p <.0001), CCL4 (One-Way ANOVA, p <.0001)) (Fig. 6B, G, H and Table 2c) and 5xFAD females (IL-6 (One-Way ANOVA, p = .0273),

CCL3 (One-Way ANOVA, p <.0001), CCL4 (One-Way ANOVA, p <.0001)) (Fig. 7B, G and Table 2d). When comparing the mRNA fold change among groups (Table 2a and b), only the two-hit 5xFAD males treated with TG11-77.HCl showed a significant decrease in cytokines and chemokines (paired t-test, $p < 0.0001$) (Fig. 8D and Table 2e).

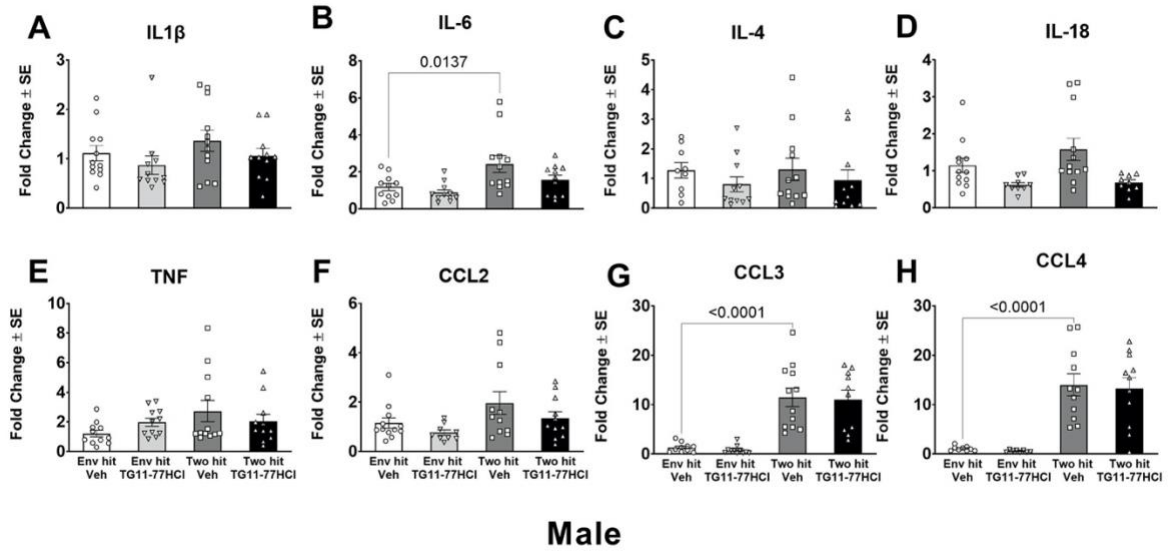

Figure 6. mRNA Fold Change of Cytokines and Chemokines (Males). (*$p < 0.5$; **$p < 0.01$; ***$p < 0.001$; ****$p < .0001$ One-way ANOVA, Dunnett's multiple comparison test Each symbol represents the mRNA fold change of an individual mouse. The bar graph represents the average of the groups. The bold horizontal bar is the mean and the vertical bars are the standard error of the mean. Env hit is the environmental hit (single hit); two hit is the environmental hit with LPS administration; veh is the vehicle for TG11-77.HCl.

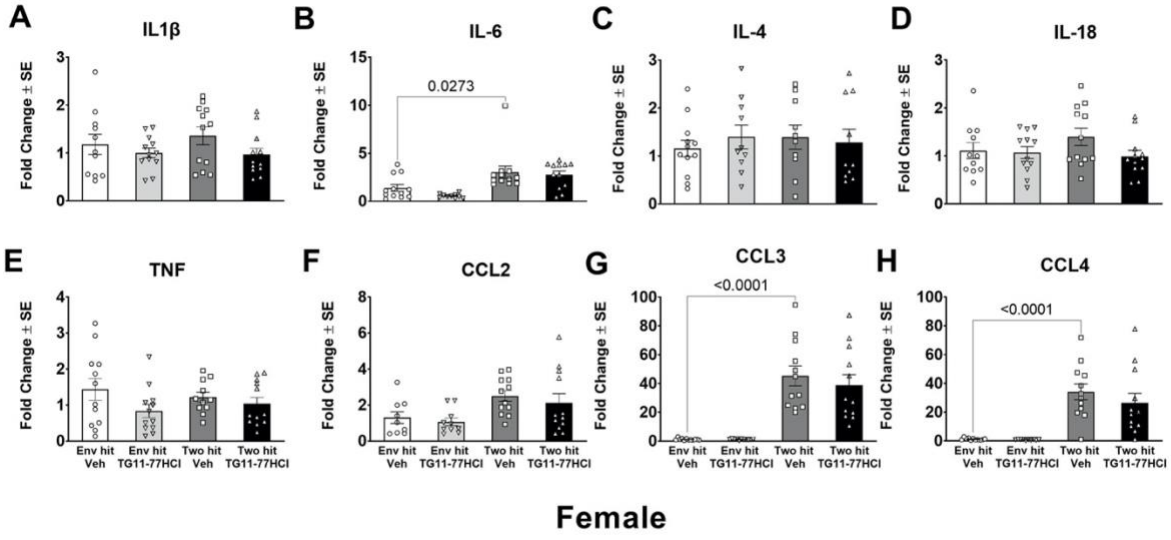

Figure 7. mRNA Fold Change of Cytokines and Chemokines (females). (*$p < 0.5$; **$p < 0.01$; ***$p < 0.001$; ****$p < .0001$ One-way ANOVA, Dunnett's multiple comparison test Each symbol represents the mRNA fold change of an individual mouse. The bar graph represents the average of the groups. The bold horizontal bar is the mean and the vertical bars are the standard error of the mean. Env hit is the environmental hit (single hit); two hit is the environmental hit with LPS administration; veh is the vehicle for TG11-77.HCl.

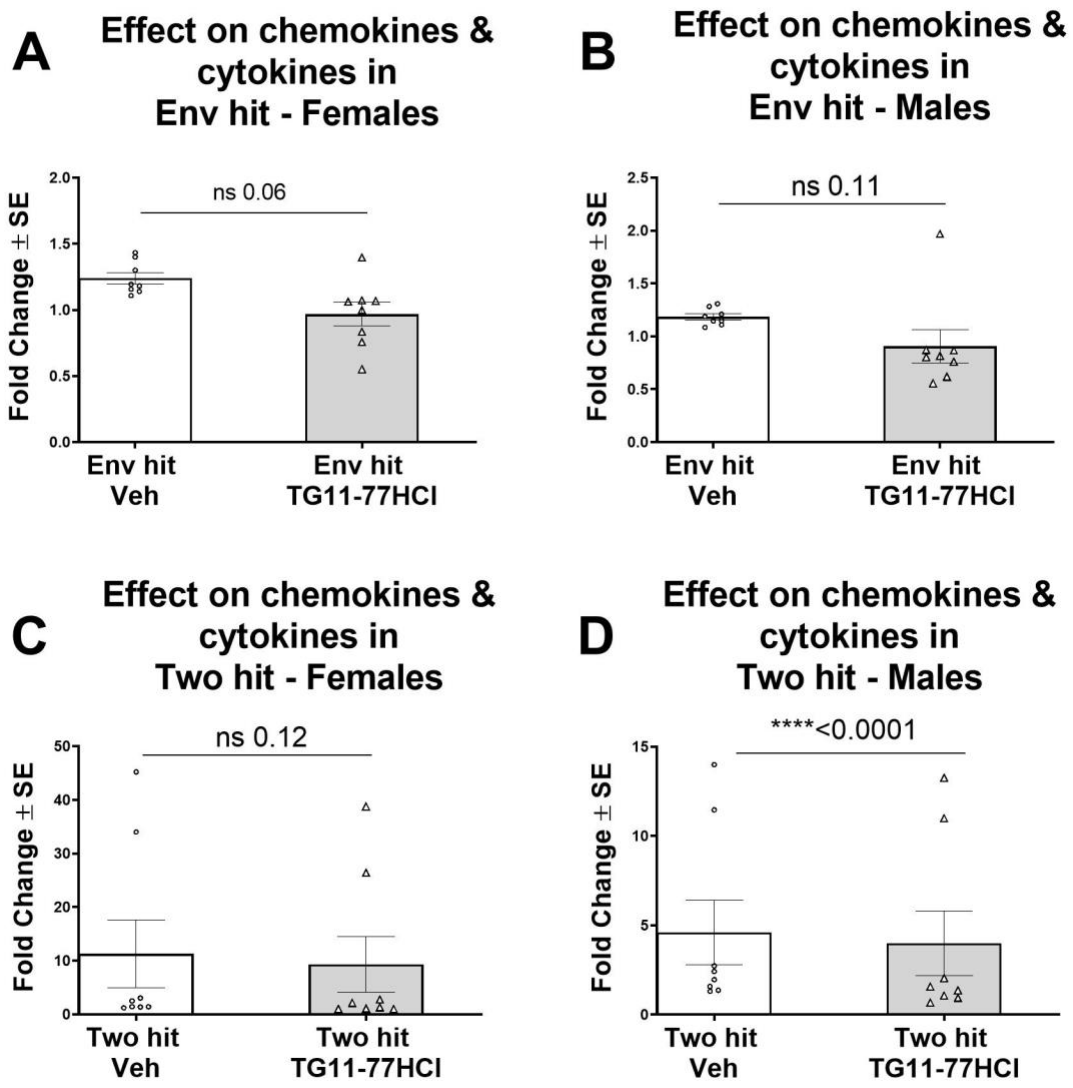

Figure 8. mRNA Fold Change Between All Cytokines and Chemokines Among Groups. (*$p < 0.5$; **$p < 0.01$; ***$p < 0.001$; paired t test). Each symbol represents the individual genes. The bar graph represents the average mRNA fold change for all genes in the group. Env hit is the environmental hit (single hit); two hit is the environmental hit with LPS administration; veh is the vehicle for TG11-77.HCl.

Gliosis

The level of mRNA for glial markers GFAP(IL-6 (One-Way ANOVA, p = .0045) CD68 6 (One-Way ANOVA, p = .0002) and CD11b 6 (One-Way ANOVA, p = .0074) were significantly upregulated in 5xFAD male mice in the two-hit model (Fig. 9A, B, D and Table 3c). In addition, there was a significant upregulation of GFAP 6 (One-Way ANOVA, p < .0001), CD68 6 (One-Way ANOVA, p = .0005) and IBA16 (One-Way ANOVA, p = .0071) in 5xFAD female mice (Fig. 10, A, B, C and Table 3d). Comparing the mRNA fold changes between the groups (Table 3a and b), the data indicates a decrease in microglial and astroglia markers for the two-hit male 5xFAD model treated with TG11-77.HCl (paired t-test, p < .05) (Fig. 11D and Table 3e) and a two-hit female 5xFAD mouse model treated with TG11-77.HCl (paired t-test, p < .01) (Fig. 11C and Table 3e).

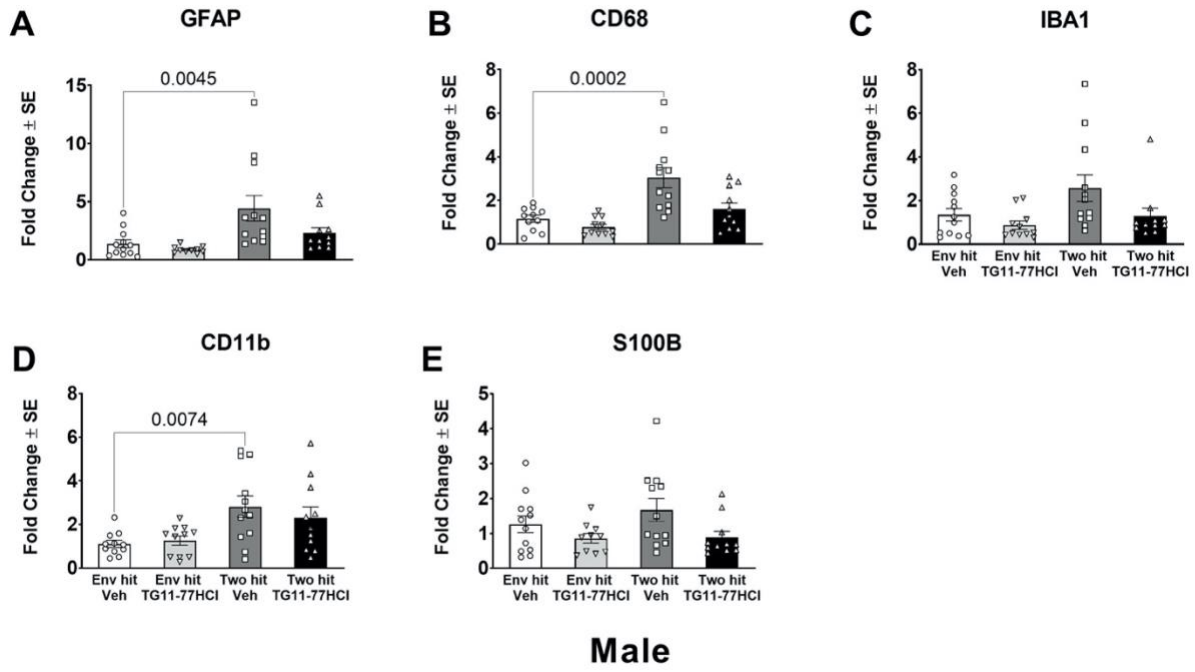

Figure 9. mRNA Fold Change of Astroglia and Microglia (Males). (*p < 0.5; **p < 0.01; ***p < 0.001; ****p < .0001 One-way ANOVA, Dunnett's multiple comparison test Each symbol represents the mRNA fold change of an individual mouse. The bar graph represents the average of the groups. The bold horizontal bar is the mean, and the vertical bars are the standard error of the

mean. Env hit is the environmental hit (single hit); two hit is the environmental hit with LPS administration; veh is the vehicle for TG11-77.HCl.

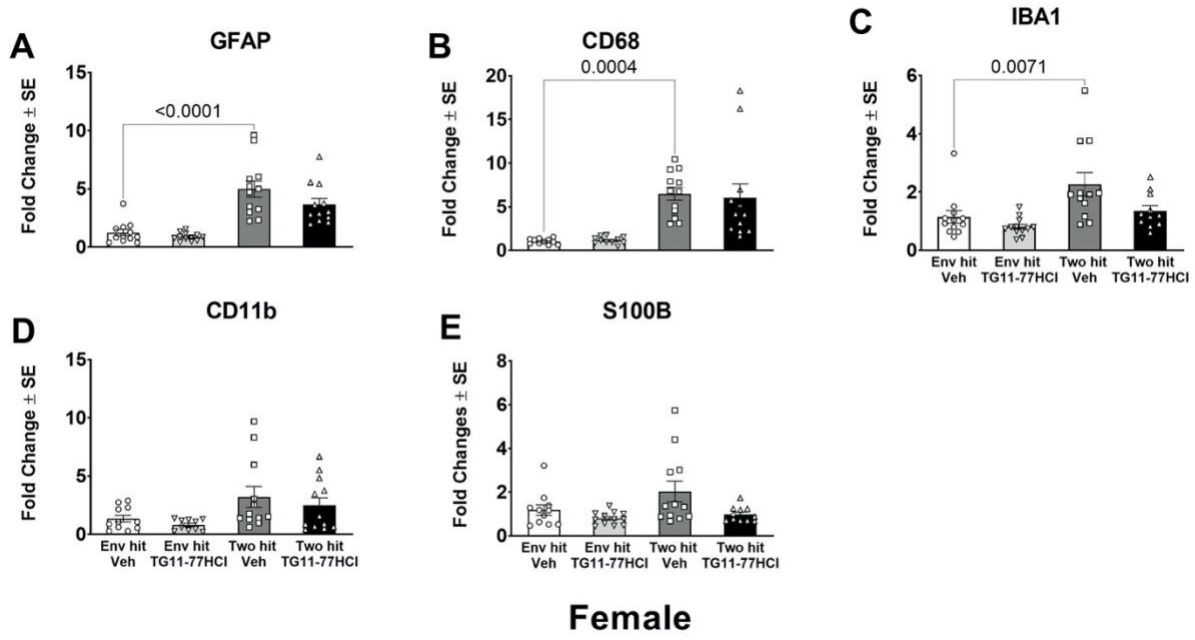

Figure 10. mRNA Fold Change of Astroglia and Microglia (females). (*$p < 0.5$; **$p < 0.01$; ***$p < 0.001$; ****$p < .0001$ One-way ANOVA, Dunnett's multiple comparison test Each symbol represents the mRNA fold change of an individual mouse. The bar graph represents the average of the groups. The bold horizontal bar is the mean, and the vertical bars are the standard error of the mean. Env hit is the environmental hit (single hit); two hit is the environmental hit with LPS administration; veh is the vehicle for TG11-77.HCl.

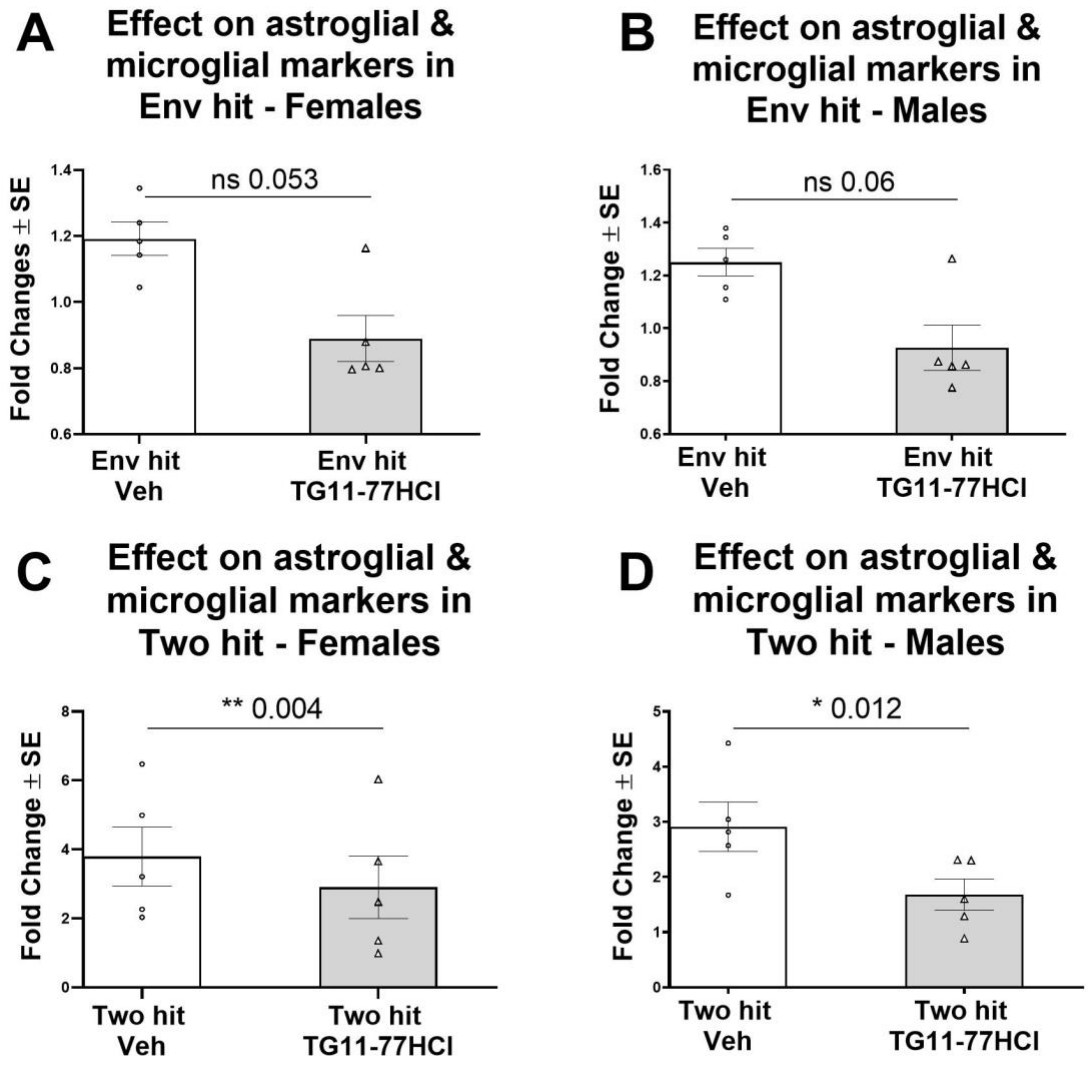

Figure 11. mRNA Fold Change Between All Astroglia and Microglia Among Groups. (*$p < 0.5$; **$p < 0.01$; ***$p < 0.001$; paired t test). Each symbol represents the individual genes. The bar graph represents the average mRNA fold change for all genes in the group. Env hit is the environmental hit (single hit); two hit is the environmental hit with LPS administration; veh is the vehicle for TG11-77.HCl.

Congo Red staining

Congo red staining was performed to visualize and quantify the overall amyloid-Aβ plaque pathology (red) that developed in the brains. As shown in Figure. 12A, 12B, and 12C, there is a reduction in those areas for male 5xFAD treated with TG11-77.HCl in the number of plaques,

average size, and percent area covered by Aβ plaques. These differences can also be visualized in select regions of the brain via staining, illustrating an attenuation of amyloid pathology in the two-hit male brain treated with TG11-77.HCl. (Fig. 13D-F)

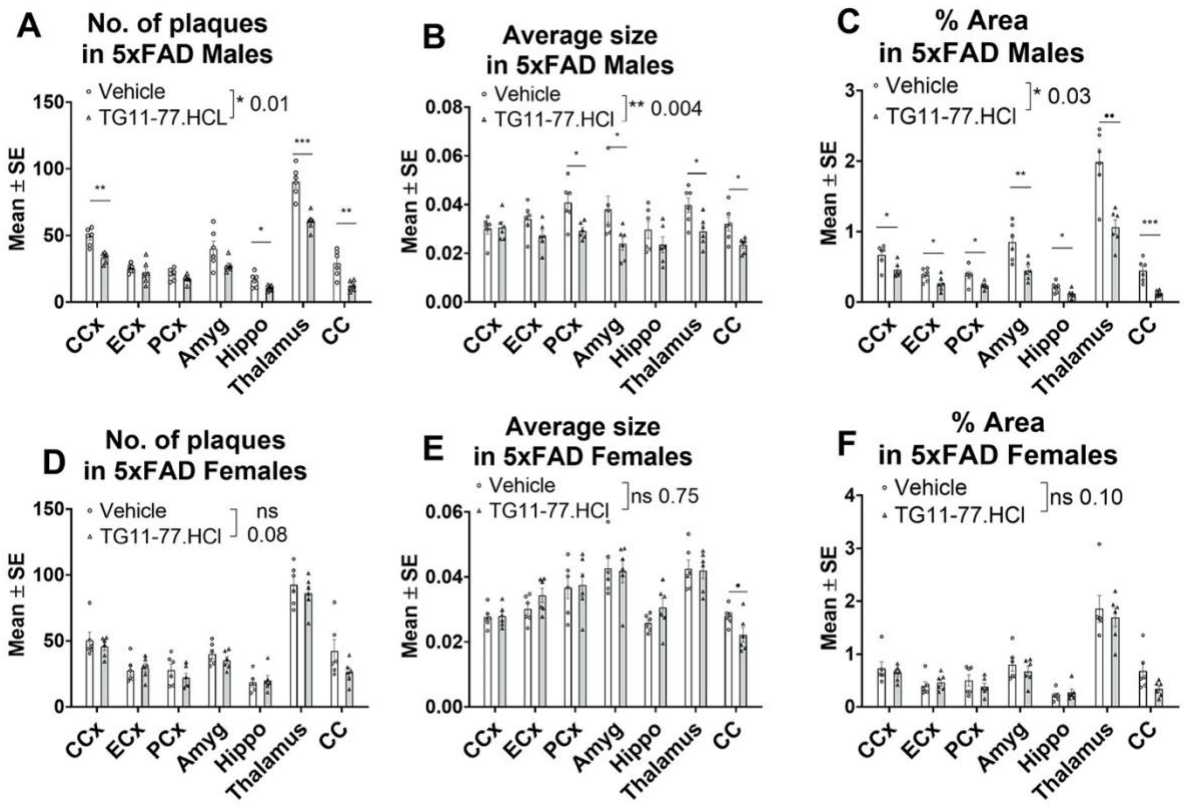

Figure 12. Mean ± SE of the number of plaques, average size, and percent area covered for individual regions in the brain of a two-hit mouse model ($p < 0.5$; $^{**}p < 0.01$; $^{***}p < 0.001$; unpaired student's t test with multiple comparisons using two stage step-up (Benjamini, Krieger, and Yekutieli) with FDR (Q) = 5%) and a group analysis between each treatment ($p < 0.5$; $^{**}p < 0.01$; $^{***}p < 0.001$; Paired t-test). Bars represents Mean ± SE, and the symbols represent individual animals.

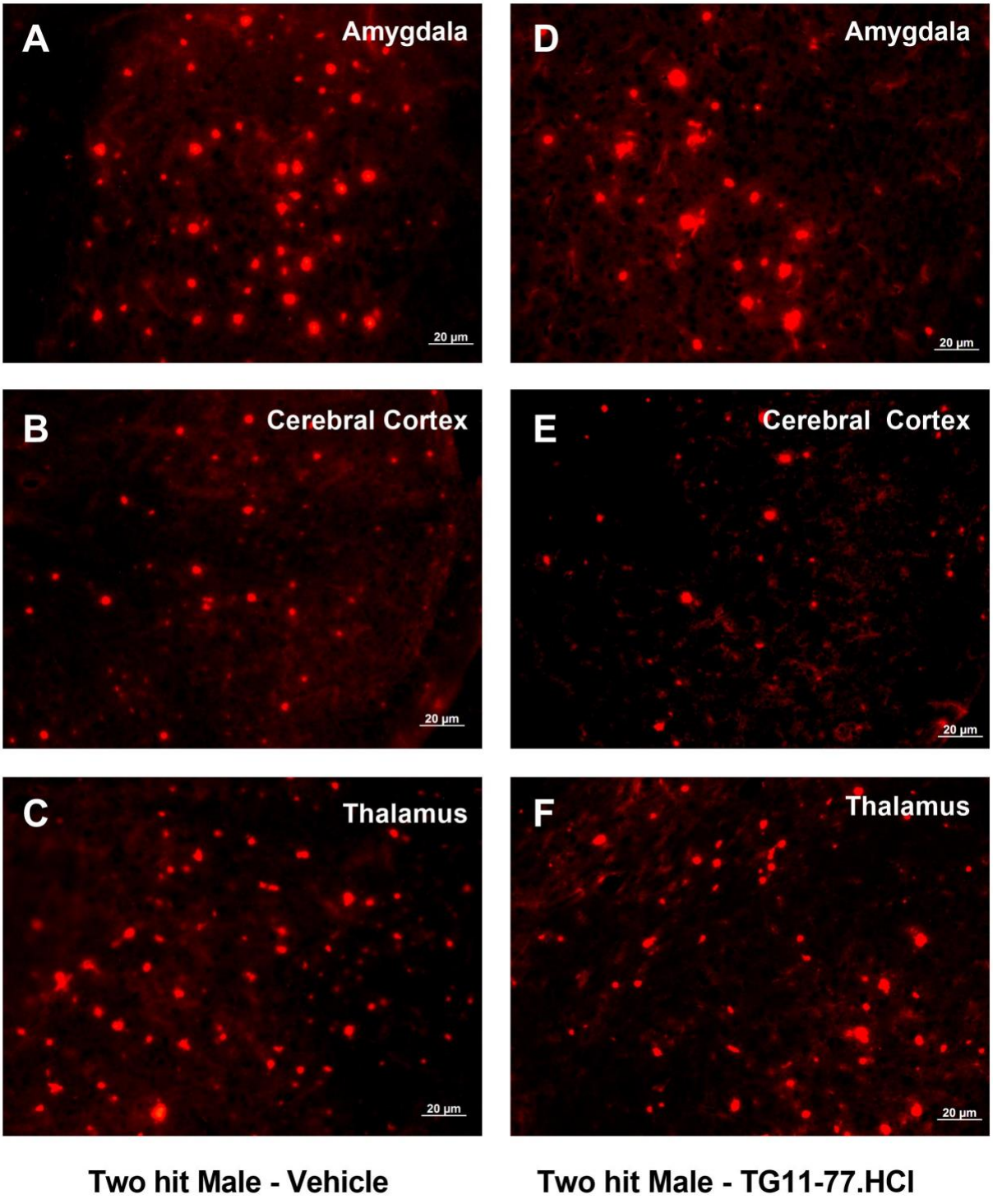

Figure 13. Congo Red Staining in a two-hit mouse model treated with vehicle or TG11-77.HCl. Bright red indicates Aβ plaques. Scale bar represents 20 µm; 30-micron thick sections were made using a freezing microtome.

GFAP Staining

GFAP staining was performed to visualize and quantify the overall number of astrocytes that accumulated in selected brain regions. A significant increase in astrocytes numbers were detected for the single-hit cohort treated with the EP2 antagonist (TG11-77.HCl) compared to the single-hit cohort treated with vehicle (Fig. 14A). Panels B and C of Figure 14 illustrates the positive staining of GFAP and the increase in astrocytes accumulation in the cerebral cortex of the single-hit groups. Panels E and F of Figure 14 illustrates positive astrocyte staining in the cerebral cortex of the two-hit groups.

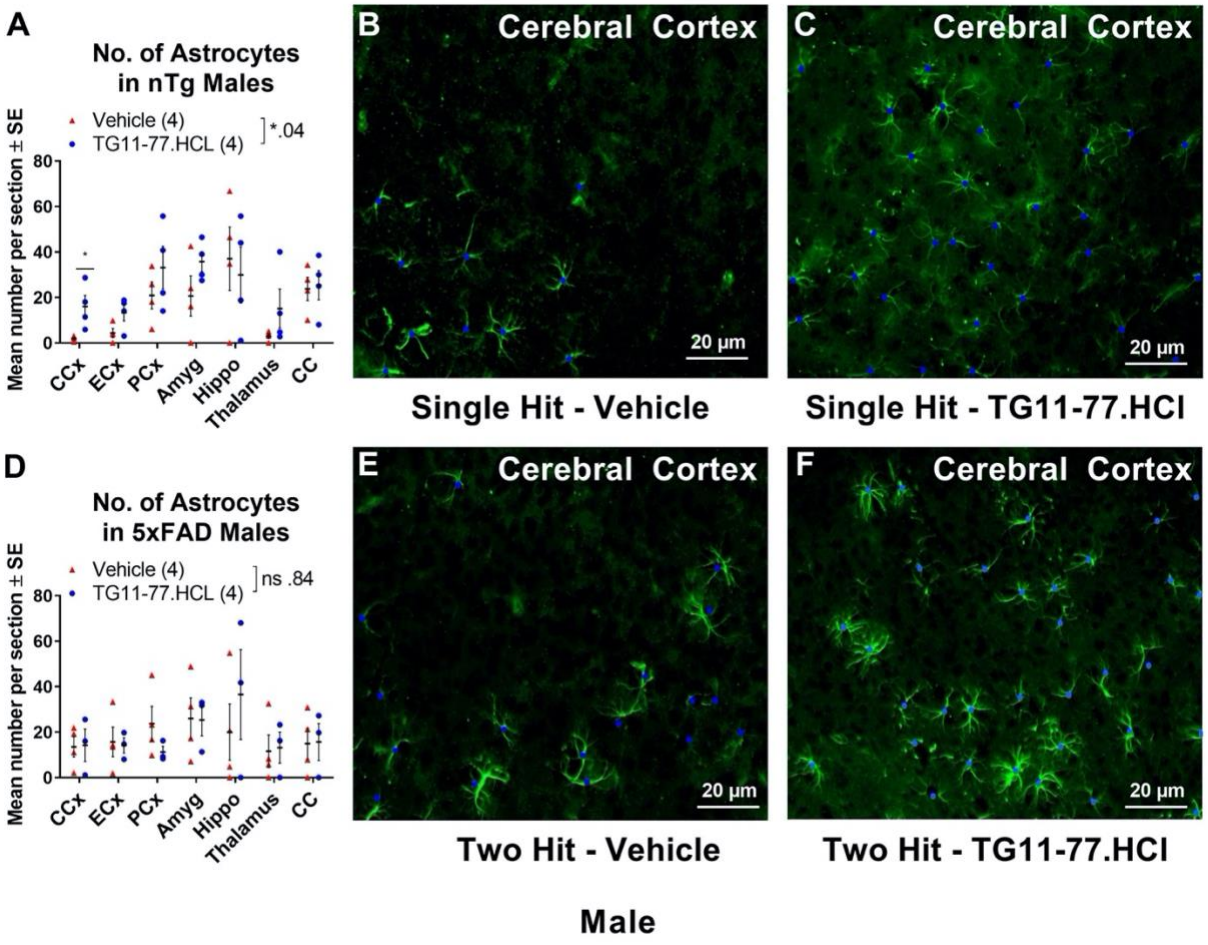

Figure 14. Mean ± SE of the number astrocytes for individual regions in the brain ($p < 0.5$; $^{**}p < 0.01$; $^{***}p < 0.001$; unpaired student's t test with multiple comparisons using two stage step-up (Benjamini, Krieger, and Yekutieli) with FDR (Q) = 5%) and a group analysis between each treatment ($p < 0.5$; $^{**}p < 0.01$; $^{***}p < 0.001$; Paired t-test). GFAP in single-hit and two-hit mouse models treated with vehicle or TG11-77.HCl. Green indicates astrocytes. The blue dots indicate the counts of the astrocytes. Scale bar represents 20 µm; 30-micron thick sections were made using a freezing microtome.

Discussion

Current drug discovery research that revolves around clinical trial designs are centered on symptomatic patients, but disease progression is often too late to show any significant efficacy of the drug. For example, therapies such as acetylcholinesterase inhibitors and memantine have shown little to modest symptomatic benefit (Golde et al., 2011). In addition, recent failures in anti-

amyloid treatment resulted in an overall decrease in clinical trials (Huang et al., 2020) and a lack of support for targeting amyloid as an effective Alzheimer's disease (AD) therapy. Considering this, several interventions, including anti-tau, anti-neuroinflammation and neuroprotection interventions, have begun to be explored further (Huang et al., 2020). The focus on neuroinflammation in AD as a potential therapeutic target has given rise to drugs that bind to different types of receptors in the brain. Shifting the paradigm from treatment of symptomatic patients to early intervention for AD therapies could help in reducing both the incidence and prevalence of clinical AD. A previous study demonstrated early inflammatory changes in the 5xFAD mouse model to occur around 3 months of age (Manji et al., 2019).

In a recent study, a two-hit inflammatory hypothesis that exhibits amyloid-β plaques and neuroinflammation externally has been explored with some therapeutic benefit of an EP2 receptor antagonist in altering disease pathology (Banik et al., 2021). In the current study, the aim was to examine the anti-inflammatory efficacy of an EP2 antagonist in a two-hit 5xFAD mice model of AD induced by an external environmental stimulus of LPS for 12 weeks starting at the asymptomatic phase (2 months of age) using 5XFAD B6SJL background mice. This asymptomatic phase is characterized by the presence of amyloid-β and gliosis (Ismeurt et al., 2020). Additionally, a cohort of 5xFAD mice and non-transgenic (nTg) mice treated with the EP2 antagonist, or the vehicle was compared to test the efficacy of the EP2 antagonist in a one-hit or two-hit model.

Studies have demonstrated both protective and deleterious roles of the EP2 receptor in disease outcome (Ganesh, 2014). As for its neuroprotective effects, inhibition of the myeloid EP2 signaling rejuvenated cellular bioenergetics, systemic and brain inflammatory states, hippocampal synaptic plasticity, and spatial memory (Minhas et al., 2021). One study demonstrated the deleterious effect in an EP2 knockout mouse, where the deletion of the EP2 receptor led to

significant cognitive and social deficits, in addition to impaired spatial learning (Savonenko et al., 2009). This study suggests that there could be an association between the EP2 receptor and learning and memory. Mechanistically, PGE_2–EP2 signaling leads to the activation of protein kinase B (AKY), which results in the phosphorylation and inactivation of GSK3β, activating glycogen synthase (GYS1) and glycogen synthesis (Minhas et al., 2021). Through the inhibition of the EP2 receptor, it will be interesting to explore the ways in which the utilization of our selective EP2 antagonist may aid in the inhibition of neuroinflammation regarding cognitive impairment in AD.

In the current study, selective gene expression was upregulated in a two-hit 5xFAD mouse model administered LPS. The neuroinflammatory changes were relatively similar in males and females, where they both displayed an upregulation of gp91phox and TREM2 in proinflammatory mediators, GFAP and CD68 in astroglia and microglia, and IL-6, CCL3, and CCL4 in cytokines and chemokines. These results indicate that a two-hit 5xFAD mice model upregulates mRNA expression of genes known to play a detrimental role in AD. In addition, the two-hit 5xFAD model induced with an environmental stimulus (LPS) revealed an elevation in brain inflammation compared to the single-hit (LPS) cohort in both males and females.

Furthermore, an anti-inflammatory effect of the EP2 antagonist, TG11-77.HCl, was exhibited in astroglia and microglia of two-hit 5xFAD males and females, as well as cytokines and chemokines in the two-hit 5xFAD males. These results suggest that there may be therapeutic effects of the EP2 antagonist in a two-hit model of AD, particularly in males, where both the external environmental stimulus and genetic hit increases brain inflammation. The suppression of EP2 mediated neuroinflammation is believed to underlie EP2 driven neuroprotection in the brain. In contrast, the EP2 antagonist treatment was not found to be effective in the single-hit model, as shown in a previous study (Banik et al., 2021).

The cAMP/Epac signaling pathway has been proposed as the mechanisms by which EP2 activation accentuates chronic inflammation (Jiang & Dingledine, 2013). This may indicate an EP2 modulation in glial activation that negatively impacts the debris clearing mechanism of microglia. The study investigated the effects of the EP2 antagonist on astrocytes by quantifying astrocyte numbers in brain regions using the astrocyte marker GFAP. There was a significant increase in astrocyte numbers shown in the cerebral cortex, in the single-hit mice treated with TG11-77.HCl compared to the single-hit mouse treated with the vehicle, suggesting that the EP2 antagonist does not reduce all features of AD pathology. However, it should be noted that the number of mice in each group was low and perhaps this apparent increase would be different if more mice were samples. The EP2 receptor is presumed to not play a direct role in astrogliosis in the AD brain as the EP2 receptor is believed to be expressed in microglia, and not astrocytes.

The study also explored the effects of the EP2 antagonist on amyloid pathology. There was statistical significance in the two-hit 5xFAD male cohort, where the use of an EP2 antagonist reduced the percent area, size, and the number of amyloid-β plaques. The data presented here reinforces the hypothesis that the inhibition of the EP2 receptor may aid in the reduction of amyloid-β levels via phagocytosis, an idea supported by another study (Fox et al., 2015).

The mechanism by which there is a reduction in neuroinflammation by TG11-77.HCl in a two-hit 5xFAD mouse model may reflect potential mechanisms of the suppression of EP2 mediated neuroinflammation. Studies have demonstrated both the protective and deleterious role of the EP2 receptor discussed in a review (Ganesh, 2014).

Though epidemiological studies have reported the reduced risk of the disorder with the use of non-steroidal anti-inflammatory drugs (NSAID), some inflammation may induce a beneficial immune response (Wyss-Coray, 2006). Targeting and inhibiting the COX-2 gene may be too broad,

resulting in issues outside of the brain, like cardiovascular side effects (Ganesh, 2014). Considering this, limitations may arise with the use of anti-inflammatory drugs, where broad inhibition of inflammation would be detrimental. Currently, treatment for AD revolves around the utilization of non-steroidal anti-inflammatory drugs (NSAIDs), which have been shown to serves as an inhibitor to the COX-2 signaling pathway (Zhang et al., 2018). There are, however, adverse effects in the later stages of AD pathogenesis (Breitner et al., 2011), and also in adverse cardiovascular side effects like myocardial infarction and stroke (Grosser et al., 2010), indicating that broad inhibition of COX-2 may have adverse effects on AD pathogenesis, and that the use of NSAIDs may not be beneficial in reducing the effects of AD pathology in the long-term treatment.

Conclusion

This study demonstrates the efficacy of an EP2 antagonist in a two-hit model consisting of a genetic 5xFAD B6SJL mouse, as well as an environmental hit of LPS comparing males and females. Results have indicated a reduction in cytokines, chemokines, astroglia and microglial markers in 5xFAD males treated with an EP2 antagonist. In addition, there seems to be an attenuation of amyloid pathology in 5xFAD males treated with the EP2 antagonist. Similarly, there was a reduction in astroglia and microglial markers in 5xFAD females treated with an EP2 antagonist. The study provides support for the hypothesis the TG11-77HCl reduces amyloid burden, as well as neuroinflammation, particularly in the 5xFAD males.

This study may indicate a potential therapeutic avenue for treatment in the prodromal stages of AD for a drug that targets downstream, mitigating any issues that arise from broad inhibition. This study can also be helpful in providing insight into a possible mechanism by which selective inhibition of inflammatory mediators exert their effects, and how it relates to neurodegenerative diseases like AD.

Future Directions

Further investigation on microglia activation would be helpful in being able to quantify brain levels of microglia using IBA1 immunostaining and possibly correlating microglia activation to other neuropathology detected in the 5xFAD mice. As the EP2 receptor is expressed in microglia, there may be a change in microgliosis following treatment of the AD mice with the EP2 antagonist (TG11-77.HCl). In addition, a more in-depth investigation of astrocyte may be worth pursuing, as the number of sections and animals used in the analysis was low (n=4). Perhaps increasing the sample size would decrease variability. Although a recent study (Banik et al., 2021) demonstrated administration of TG-1177HCl in a two-hit 5xFAD model had anti-inflammatory properties that triggered EP2 derived neuroinflammation in the AD brain, the paper did not demonstrate any benefit to the amyloid burden. Therefore, it would be interesting to investigate the tau pathology to determine if this early therapeutic strategy involving EP2 antagonism is beneficial regarding the buildup of tau. Furthermore, in the future it may be important to explore an optimization of the treatment paradigm at varying ages of the disease progression using a 5xFAD B6SJL model with TG11-77HCl. Exploring the efficacy of the drug after the prodromal stage will help in understanding the disease progression at different stages of AD. This can also give insight into the pathways involved in triggering neuroinflammation and related pathophysiology in the two-hit model of AD.

Limitations

One limitation in this study is the general availability of mouse models with neuroinflammation that can translate to clinical cases of AD. Though the 5xFAD mouse model is a model that has human FAD mutations and develops amyloid-β plaques, it does not develop neurofibrillary tangles. Therefore, there are components that are like clinical AD, but it cannot

fully mirror AD pathology in humans**.** In addition, the troubleshooting process of the GFAP stain was a limitation in this project. Due to various technical problems with the sections and the immunostaining technique, as well as visualization of the astrocytes, there were difficulties in obtaining data. Though we investigated the effects of TG11-77.HCl on astrogliosis, the effects of the EP2 antagonist on microgliosis in the AD brain have not been explored in the two hit model with the B6SJL background. This may be a limitation regarding the conclusion made with the EP2 antagonist and its effects on gliosis.

Appendix

Table 1a. Mean mRNA fold changes with standard deviations of proinflammatory mediators for one-hit and two-hit mouse models treated with vehicle or TG11-77.HCl in males.

Genes	nTg Veh Male (n = 12)		nTg TG11-77 Male (n = 12)		5XFAD Veh Male (n = 12)		5xFAD TG11-77 Male (n = 12)	
	Mean	SD	Mean	SD	Mean	SD	Mean	SD
EP2	1.147	0.616	5.465	8.353	2.879	2.583	2.402	3.276
COX-2	1.195	0.885	0.941	0.317	1.472	1.084	0.841	0.402
p47phox	1.261	0.844	0.958	0.536	2.186	1.419	1.007	0.445
gp91phox	1.166	0.607	0.841	0.211	3.503	1.982	1.576	0.408
iNOS	1.285	0.811	0.637	0.310	1.164	0.425	0.758	0.408
TREM2	1.255	0.828	1.208	0.775	6.867	5.249	2.782	1.214

Table 1b. Mean mRNA fold changes with standard deviations of proinflammatory mediators for one-hit and two-hit mouse models treated with vehicle or TG11-77.HCl in females.

Genes	nTg Veh Female (n = 12)		nTg TG11-77 Female (n = 12)		5xFAD Veh Female (n = 12)		5xFAD TG11-77 Female (n = 12)	
	Mean	SD	Mean	SD	Mean	SD	Mean	SD
EP2	1.154	0.707	1.257	1.042	2.247	1.911	1.804	1.960
COX-2	1.266	0.841	0.947	0.427	1.071	0.451	0.896	0.370
p47phox	1.197	0.701	0.825	0.315	1.914	1.056	1.491	0.563
gp91phox	1.117	0.587	1.032	0.451	2.660	0.716	3.449	1.749
iNOS	1.025	0.236	1.160	0.422	1.528	0.632	1.427	1.749
TREM2	1.221	0.836	0.717	0.330	5.862	3.191	4.812	1.574

Table 1c. Mean differences in mRNA fold changes with 95% Confidence Interval of proinflammatory mediators between one-hit mouse model treated with vehicle, and one-hit treated with TG11-77.HCl, or two-hit mouse models treated with vehicle or TG11-77.HCl in males (*p < 0.5; **p < 0.01; ***p < 0.001; ****p < .0001 1-way ANOVA, Dunnett's multiple comparison test).

Genes	nTg Veh vs nTg TG11-77 Male (n = 12)		nTg Veh vs 5XFAD Veh Male (n = 12)		nTg Veh vs 5XFAD TG11-77 Male (n = 12)	
	Mean diff	95.00 CI	Mean diff	95.00 CI	Mean diff	95.00 CI
EP2	-4.318	-9.989, 1.353	-1.732	-7.521, 4.057	-1.256	-7.186, 4.674
COX-2	0.254	-0.519, 1.026	-0.278	-1.033, 0.478	0.354	-0.419, 1.127
p47phox	0.303	-0.681, 1.286	-0.925	-1.889, 0.039	0.254	-0.753, 1.260
gp91phox	0.326	-0.870, 1.521	-2.337****	-3.479, -1.195	-0.410	-1.605, 0.786
iNOS	0.648*	0.094, 1.202	0.121	-0.419, 0.661	0.527	-0.027, 1.081
TREM2	0.047	-2.940, 3.034	-5.613****	-8.537, -2.689	-1.528	-4.589, 1.533

Table 1d. Mean differences in mRNA fold changes with 95% Confidence Interval of proinflammatory mediators between one-hit mouse model treated with vehicle, and one-hit treated with TG11-77.HCl, or two-hit mouse models treated with vehicle or TG11-77.HCl in males (*p < 0.5; **p < 0.01; ***p < 0.001; ****p < .0001 1-way ANOVA, Dunnett's multiple comparison test).

Genes	nTg Veh vs nTg TG11-77 Female (n = 12)		nTg Veh vs 5XFAD Veh Female (n = 12)		nTg Veh vs 5XFAD TG11-77 Female (n = 12)	
	Mean diff	95.00 CI	Mean diff	95.00 CI	Mean diff	95.00 CI
EP2	-0.103	-1.660, 1.454	-1.093	-2.650, 0.464	-0.650	-2.245, 0.946
COX-2	0.319	-0.232, 0.870	0.195	-0.356, 0.746	0.370	-0.181, 0.921
p47phox	0.371	-0.334, 1.078	-0.718*	-1.424, -0.012	-0.294	-1.001, 0.412
gp91phox	0.085	-0.930, 1.100	-1.544**	-2.582, -0.505	-2.332****	-3.347, -1.316
iNOS	-0.134	-0.709, 0.440	-0.503	-1.077, 0.071	-0.402	-0.964, 0.160
TREM2	0.503	-1.319, 2.326	-4.641****	-6.463, -2.818	-3.591****	-5.414, -1.769

Table 1e. P-values using mean differences of all proinflammatory mediators in males and females (*p < 0.5; **p < 0.01; ***p < 0.001; paired t test).

Paired T-Test	Male	Female
Env hit - Veh vs. TG11-77	.5817	.168
Two hit - Veh vs. TG11-77	.0533	.3845

Table 2a. Mean mRNA fold changes with standard deviations of cytokines and chemokines for one-hit and two-hit mouse models treated with vehicle or TG11-77.HCl in males.

Genes	nTg Veh Male (n = 12)		nTg TG11-77 Male (n = 12)		5XFAD Veh Male (n = 12)		5xFAD TG11-77 Male (n = 12)	
	Mean	SD	Mean	SD	Mean	SD	Mean	SD
IL-1ß	1.108	0.540	0.866	0.624	1.363	0.744	1.060	0.500
Il-6	1.185	0.661	0.872	0.509	2.421	1.574	1.570	0.816
IL-4	1.281	0.784	0.803	0.842	1.305	1.302	0.936	1.170
IL-18	1.145	0.667	0.617	0.193	1.576	1.045	0.675	0.226
TNF	1.209	0.762	1.968	0.924	2.722	2.487	2.038	0.226
CCL2	1.148	0.720	0.759	0.328	1.961	1.538	1.351	0.852
CCL3	1.307	0.959	0.813	0.825	11.463	6.509	10.988	6.100
CCL4	1.084	0.483	0.555	0.222	13.983	7.390	13.249	7.411

Table 2b. Mean mRNA fold changes with standard deviations of cytokines and chemokines for one-hit and two-hit mouse models treated with vehicle or TG11-77.HCl in females.

Genes	nTg Veh Female (n = 12)		nTg TG11-77 Female (n = 12)		5XFAD Veh Female (n = 12)		5xFAD TG11-77 Female (n = 12)	
	Mean	SD	Mean	SD	Mean	SD	Mean	SD
IL-1ß	1.180	0.705	0.999	0.357	1.359	0.644	0.965	0.459
Il-6	1.401	1.216	0.551	0.219	3.028	2.231	2.760	1.366
IL-4	1.157	0.604	1.396	0.780	1.392	0.786	1.278	0.875
IL-18	1.109	0.547	1.067	0.438	1.398	0.628	0.988	0.424
TNF	1.432	1.049	0.833	0.639	1.214	0.455	1.037	0.424
CCL2	1.300	0.982	1.062	0.682	2.503	1.027	2.114	1.753
CCL3	1.140	0.669	1.071	0.339	45.200	24.095	38.744	25.314
CCL4	1.193	0.771	0.757	0.268	34.017	19.067	26.368	23.117

Table 2c. Mean differences in mRNA fold changes with 95% Confidence Interval of cytokines and chemokines between one-hit mouse model treated with vehicle, and one-hit treated with TG11-77.HCl, or two-hit mouse models treated with vehicle or TG11-77.HCl in males (*$p < 0.5$; **$p < 0.01$; ***$p < 0.001$; ****$p < .0001$ 1-way ANOVA, Dunnett's multiple comparison test).

Genes	nTg Veh vs nTg TG11-77 Male (n = 12)		nTg Veh vs 5XFAD Veh Male (n = 12)		nTg Veh vs 5XFAD TG11-77 Male (n = 12)	
	Mean diff	95.00 CI	Mean diff	95.00 CI	Mean diff	95.00 CI
IL-1ß	0.242	-0.381, 0.865	-0.254	-0.863, 0.355	0.049	-0.574, 0.671
Il-6	0.314	-0.724, 1.352	-1.235*	-2.251, -0.220	-0.385	-1.423, 0.653
IL-4	0.479	-0.687, 1.644	-0.023	-1.167, 1.120	0.345	-0.820, 1.510
IL-18	0.527	-0.2100, 1.265	-0.431	-1.114, 0.251	0.469	-0.268, 1.207
TNF	-0.759	-2.433, 0.915	-1.513	-3.152, 0.126	-0.830	-2.504, 0.845
CCL2	0.388	-0.672, 1.448	-0.814	-1.817, 0.1900	-0.203	-1.206, 0.801
CCL3	0.4938	-4.381, 5.369	-10.16***	-14.93, -5.379	-9.681****	-14.67, -4.692
CCL4	0.528	-6.139, 7.196	-12.9****	-19.07, -6.732	-12.17****	-18.33, -5.998

Table 2d. Mean differences in mRNA fold changes with 95% Confidence Interval of cytokines and chemokines between one-hit mouse model treated with vehicle, and one-hit treated with TG11-77.HCl, or two-hit mouse models treated with vehicle or TG11-77.HCl in females (*$p < 0.5$; **$p < 0.01$; ***$p < 0.001$; ****$p < .0001$ 1-way ANOVA, Dunnett's multiple comparison test).

Genes	nTg Veh vs nTg TG11-77 Female (n = 12)		nTg Veh vs 5XFAD Veh Female (n = 12)		nTg Veh vs 5XFAD TG11-77 Female (n = 12)	
	Mean diff	95.00 CI	Mean diff	95.00 CI	Mean diff	95.00 CI
IL-1ß	0.182	-0.381, 0.745	-0.178	-0.741, 0.385	0.215	-0.348, 0.778
Il-6	0.850	-0.696, 2.396	-1.628*	-3.102, -0.154	-1.359	-2.833, 0.115
IL-4	-0.239	-1.038, 0.560	-0.235	-1.034, 0.564	-0.121	-0.920, 0.678
IL-18	0.042	-0.481, 0.565	-0.290	-0.813, 0.233	0.120	-0.403, 0.643
TNF	0.599	-0.125, 1.323	0.218	-0.523, 0.958	0.395	-0.329, 1.119
CCL2	0.238	-1.116, 1.592	-1.202	-2.502, 0.097	-0.814	-2.114, 0.4857
CCL3	0.06898	-17.91, 18.05	-44.06****	-61.65, -26.47	-37.6****	-55.19, -20.02
CCL4	0.436	-16.10, 16.98	-32.82****	-48.62, -17.02	-25.18**	-40.98, -9.374

Table 2e. P-values using mean differences of all cytokines and chemokines in males and females (*$p < 0.5$; **$p < 0.01$; ***$p < 0.001$; paired t test).

Paired T-Test	Male	Female
Env hit - Veh vs. TG11-77	.1124	.0608
Two hit - Veh vs. TG11-77	****	.1181

Table 3a. Mean mRNA fold changes with standard deviations of astroglia and microglial markers for one-hit and two-hit mouse models treated with vehicle or TG11-77.HCl in males.

Genes	nTg Veh Male (n = 12)		nTg TG11-77 Male (n = 12)		5XFAD Veh Male (n = 12)		5xFAD TG11-77 Male (n = 12)	
	Mean	SD	Mean	SD	Mean	SD	Mean	SD
GFAP	1.379	1.163	0.863	0.287	4.424	3.823	2.307	1.510
CD68	1.155	0.531	0.775	0.419	3.042	1.599	1.603	0.929
IBA1	1.345	0.991	0.875	0.639	2.569	2.100	1.290	1.205
CD11b	1.109	0.536	1.264	0.690	2.816	1.706	2.300	1.655
S100B	1.260	0.834	0.857	0.438	1.670	1.119	0.886	1.655

Table 3b. Mean mRNA fold changes with standard deviations of astroglia and microglial markers for one-hit and two-hit mouse models treated with vehicle or TG11-77.HCl in females.

Genes	nTg Veh Female (n = 12)		nTg TG11-77 Female (n = 12)		5XFAD Veh Female (n = 12)		5xFAD TG11-77 Female (n = 12)	
	Mean	SD	Mean	SD	Mean	SD	Mean	SD
GFAP	1.240	0.930	0.879	0.344	4.991	2.428	3.655	1.744
CD68	1.044	0.313	1.163	0.399	6.480	2.570	6.038	5.491
IBA1	1.142	0.747	0.806	0.309	2.262	1.374	1.352	0.592
CD11b	1.344	0.985	0.800	0.483	3.208	3.063	2.481	2.254
S100B	1.184	0.789	0.796	0.292	2.027	1.644	0.981	2.254

Table 3c. Mean differences in mRNA fold changes with 95% Confidence Interval of astroglia and microglial markers between one-hit mouse model treated with vehicle, and one-hit treated with TG11-77.HCl, or two-hit mouse models treated with vehicle or TG11-77.HCl in males (*$p < 0.5$; **$p < 0.01$; ***$p < 0.001$; ****$p < .0001$ 1-way ANOVA, Dunnett's multiple comparison test).

Genes	nTg Veh vs nTg TG11-77 Male (n = 12)		nTg Veh vs 5XFAD Veh Male (n = 12)		nTg Veh vs 5XFAD TG11-77 Male (n = 12)	
	Mean diff	95.00 CI	Mean diff	95.00 CI	Mean diff	95.00 CI
GFAP	0.517	-1.790, 2.823	-3.045**	-5.244, -0.846	-0.928	-3.176, 1.321
CD68	0.379	-0.664, 1.423	-1.888***	-2.909, -0.866	-0.448	-1.492, 0.595
IBA1	0.470	-0.917, 1.857	-1.224	-2.581, 0.1325	0.054	-1.333, 1.441
CD11b	-0.155	-1.484, 1.174	-1.707**	-3.008, -0.406	-1.191	-2.520, 0.1380
S100B	0.403	-0.433, 1.239	-0.410	-1.207, 0.387	0.375	-0.440, 1.189

Table 3d. Mean differences in mRNA fold changes with 95% Confidence Interval of astroglia and microglial markers between one-hit mouse model treated with vehicle, and one-hit treated with TG11-77.HCl, or two-hit mouse models treated with vehicle or TG11-77.HCl in females (*$p < 0.5$; **$p < 0.01$; ***$p < 0.001$; ****$p < .0001$ 1-way ANOVA, Dunnett's multiple comparison test).

Genes	nTg Veh vs nTg TG11-77 Female (n = 12)		nTg Veh vs 5XFAD Veh Female (n = 12)		nTg Veh vs 5XFAD TG11-77 Female (n = 12)	
	Mean diff	95.00 CI	Mean diff	95.00 CI	Mean diff	95.00 CI
GFAP	0.361	-1.203, 1.925	-3.751****	-5.315, -2.187	-2.415**	-3.979, -0.851
CD68	-0.119	-3.349, 3.112	-5.435***	-8.598, -2.273	-4.993**	-8.156, -1.831
IBA1	0.336	-0.515, 1.187	-1.12**	-1.971, -0.269	-0.210	-1.080, 0.661
CD11b	0.544	-1.630, 2.719	-1.863	-3.941, 0.215	-1.136	-3.214, 0.941
S100B	0.387	-0.580, 1.354	-0.843	-1.810, 0.124	0.203	-0.785, 1.191

Table 3e. P-values using mean differences of all astroglia and glial markers in males and females (*$p < 0.5$; **$p < 0.01$; ***$p < 0.001$; paired t test).

Paired T-Test	Male	Female
Env hit - Veh vs. TG11-77	.0571	.0533
Two hit - Veh vs. TG11-77	.0115*	.004**

Table 4. PCR primer sequences

Genes	Forward Primer (sequence 5'-3')	Reverse Primer (sequence 5'-3')
GAPDH	TGTCCGTCGTGGATCTGAC	CCTGCTTCACCACCTTCTTG
β-Actin	AAGGCCAACCGTGAAAAGAT	GTGGTACGACCAGAGGCATAC
HPRT	GGAGCGGTAGCACCTCCT	CTGGTTCATCATCGCTAATCAC
EP2 (PTGER2)	TCTTTAGTCTGGCCACGATGCTCA	GCAGGGAACAGAAGAGCAAGGAGG
COX-2	ACCAACGCTGCCACAACT	GGTTGGAACAGCAAGGATTT
p47phox	CAGCCATGGGGGACACCTTCATT	GCCTCAATGGGGAACATCTCCTTCA
gp91phox	TGCCACCAGTCTGAAACTCA	GCATCTGGGTCTCCAGCA
iNOS	CCTGGAGACCCACACACTG	CCATGATGGTCACATTCTGC
TREM2	GGTGCCATGGGACCTCTCCACCAGTTT	CTTCAGAGTGATGGTGACGGTTCCAGC
IL-1β (IL1B)	CAGGAAGGCAGTGTCACTCA	TCCCACGAGTCACAGAGGA
IL-6 (IL6)	AACTCCATCTGCCCTTCAGGAACA	AAGGCAGTGGCTGTCAACAACATC
IL-4	GGTCTCAACCCCCAGCTAGT	GCCGATGATCTCTCTCAAGTGAT
IL-18	GACTCTTGCGTCAACTTCAAGG	CAGGCTGTCTTTTGTCAA
TNF-α (TNF)	TCTTCTGTCTACTGAACTTCGG	AAGATGATCTGAGTGTGAGGG
CCL2	CATCCACGTGTTGGCTCA	GCTGCTGGTGATCCTCTTGTA
CCL3	TGCCCTTGCTGTTCTTCTCT	GTGGAATCTTCCGGCTGTAG
CCL4	CATGAAGCTCTGCGTGTCTG	GGAGGGTCAGAGCCCATT
GFAP	GACAACTTTGCACAGGACCTC	ATACGCAGCCAGGTTGTTCT
CD68	CTCTCTAAGGCTACAGGCTGCT	TCACGGTTGCAAGAGAAACA
Iba1	GGATTTGCAGGGAGGAAAAG	TGGGATCATCGAGGAATTG
CD11b	CCAGTAAGGTCATACAGCATCAGT	TTGATCTGAACAGGGATCCAG
S100B	TCGGACACTGAAGCCAGAG	AGACATCAATGAGGGCAACC

References

2021 Alzheimer's disease facts and figures. (2021). *Alzheimer's & Dementia*, *17*(3), 327–406. https://doi.org/10.1002/alz.12328

Alonso, A. D., Cohen, L. S., Corbo, C., Morozova, V., ElIdrissi, A., Phillips, G., & Kleiman, F. E. (2018). Hyperphosphorylation of Tau Associates With Changes in Its Function Beyond Microtubule Stability. *Frontiers in Cellular Neuroscience*, *12*, 338. https://doi.org/10.3389/fncel.2018.00338

Amaradhi, R., Banik, A., Mohammed, S., Patro, V., Rojas, A., Wang, W., Motati, D. R., Dingledine, R., & Ganesh, T. (2020). Potent, Selective, Water Soluble, Brain-Permeable EP2 Receptor Antagonist for Use in Central Nervous System Disease Models. *Journal of Medicinal Chemistry*, *63*(3), 1032–1050. https://doi.org/10.1021/acs.jmedchem.9b01218

Azizi, G., Khannazer, N., & Mirshafiey, A. (2014). The Potential Role of Chemokines in Alzheimer's Disease Pathogenesis. *American Journal of Alzheimer's Disease & Other Dementias®*, *29*(5), 415–425. https://doi.org/10.1177/1533317513518651

Azizi, G., Navabi, S. S., Al-Shukaili, A., Seyedzadeh, M. H., Yazdani, R., & Mirshafiey, A. (2015). The Role of Inflammatory Mediators in the Pathogenesis of Alzheimer's Disease. *Sultan Qaboos University Medical Journal*, *15*(3), e305–e316. https://doi.org/10.18295/squmj.2015.15.03.002

Bancher, C., Braak, H., Fischer, P., & Jellinger, K. A. (1993). Neuropathological staging of Alzheimer lesions and intellectual status in Alzheimer's and Parkinson's disease patients. *Neuroscience Letters*, *162*(1), 179–182. https://doi.org/10.1016/0304-3940(93)90590-H

Banik, A., Amaradhi, R., Lee, D., Sau, M., Wang, W., Dingledine, R., & Ganesh, T. (2021). Prostaglandin EP2 receptor antagonist ameliorates neuroinflammation in a two-hit mouse

model of Alzheimer's disease. *Journal of Neuroinflammation*, *18*, 273. https://doi.org/10.1186/s12974-021-02297-7

Batista, C. R. A., Gomes, G. F., Candelario-Jalil, E., Fiebich, B. L., & de Oliveira, A. C. P. (2019). Lipopolysaccharide-Induced Neuroinflammation as a Bridge to Understand Neurodegeneration. *International Journal of Molecular Sciences*, *20*(9), 2293. https://doi.org/10.3390/ijms20092293

Breitner, J. C., Baker, L. D., Montine, T. J., Meinert, C. L., Lyketsos, C. G., Ashe, K. H., Brandt, J., Craft, S., Evans, D. E., Green, R. C., Ismail, M. S., Martin, B. K., Mullan, M. J., Sabbagh, M., Tariot, P. N., & ADAPT Research Group. (2011). Extended results of the Alzheimer's disease anti-inflammatory prevention trial. *Alzheimer's & Dementia: The Journal of the Alzheimer's Association*, *7*(4), 402–411. https://doi.org/10.1016/j.jalz.2010.12.014

Bronzuoli, M. R., Iacomino, A., Steardo, L., & Scuderi, C. (2016). Targeting neuroinflammation in Alzheimer’s disease. *Journal of Inflammation Research*, *9*, 199–208. https://doi.org/10.2147/JIR.S86958

Chatterjee, P., Pedrini, S., Stoops, E., Goozee, K., Villemagne, V. L., Asih, P. R., Verberk, I. M. W., Dave, P., Taddei, K., Sohrabi, H. R., Zetterberg, H., Blennow, K., Teunissen, C. E., Vanderstichele, H. M., & Martins, R. N. (2021). Plasma glial fibrillary acidic protein is elevated in cognitively normal older adults at risk of Alzheimer's disease. *Translational Psychiatry*, *11*(1), 1–10. https://doi.org/10.1038/s41398-020-01137-1

Chow, V. W., Mattson, M. P., Wong, P. C., & Gleichmann, M. (2010). An Overview of APP Processing Enzymes and Products. *Neuromolecular Medicine*, *12*(1), 1–12. https://doi.org/10.1007/s12017-009-8104-z

Cristóvão, J. S., & Gomes, C. M. (2019). S100 Proteins in Alzheimer's Disease. *Frontiers in Neuroscience, 13*. https://www.frontiersin.org/article/10.3389/fnins.2019.00463

Dai, M.-H., Zheng, H., Zeng, L.-D., & Zhang, Y. (2017). The genes associated with early-onset Alzheimer's disease. *Oncotarget*, *9*(19), 15132–15143. https://doi.org/10.18632/oncotarget.23738

DeTure, M. A., & Dickson, D. W. (2019). The neuropathological diagnosis of Alzheimer's disease. *Molecular Neurodegeneration*, *14*(1), 32. https://doi.org/10.1186/s13024-019-0333-5

Fox, B. M., Beck, H. P., Roveto, P. M., Kayser, F., Cheng, Q., Dou, H., Williamson, T., Treanor, J., Liu, H., Jin, L., Xu, G., Ma, J., Wang, S., & Olson, S. H. (2015). A selective prostaglandin E2 receptor subtype 2 (EP2) antagonist increases the macrophage-mediated clearance of amyloid-beta plaques. *Journal of Medicinal Chemistry*, *58*(13), 5256–5273. https://doi.org/10.1021/acs.jmedchem.5b00567

Franco-Bocanegra, D. K., George, B., Lau, L. C., Holmes, C., Nicoll, J. A. R., & Boche, D. (2019). Microglial motility in Alzheimer's disease and after Aβ42 immunotherapy: A human post-mortem study. *Acta Neuropathologica Communications*, *7*(1), 174. https://doi.org/10.1186/s40478-019-0828-x

Ganesh, T. (2014a). Prostanoid Receptor EP2 as a Therapeutic Target. *Journal of Medicinal Chemistry*, *57*(11), 4454–4465. https://doi.org/10.1021/jm401431x

Ganesh, T. (2014b). Prostanoid Receptor EP2 as a Therapeutic Target. *Journal of Medicinal Chemistry*, *57*(11), 4454–4465. https://doi.org/10.1021/jm401431x

Golde, T. E., Schneider, L. S., & Koo, E. H. (2011). Anti-Aβ therapeutics in Alzheimer's disease: The Need for a Paradigm Shift. *Neuron*, *69*(2), 203–213. https://doi.org/10.1016/j.neuron.2011.01.002

Gong, P., Chen, Y., Lin, A., Zhang, H., Zhang, Y., Ye, R. D., & Yu, Y. (2020). P47phox deficiency improves cognitive impairment and attenuates tau hyperphosphorylation in mouse models of AD. *Alzheimer's Research & Therapy*, *12*, 146. https://doi.org/10.1186/s13195-020-00714-2

González-Reyes, R. E., Nava-Mesa, M. O., Vargas-Sánchez, K., Ariza-Salamanca, D., & Mora-Muñoz, L. (2017). Involvement of Astrocytes in Alzheimer's Disease from a Neuroinflammatory and Oxidative Stress Perspective. *Frontiers in Molecular Neuroscience*, *10*. https://www.frontiersin.org/article/10.3389/fnmol.2017.00427

Gratuze, M., Leyns, C. E. G., & Holtzman, D. M. (2018). New insights into the role of TREM2 in Alzheimer's disease. *Molecular Neurodegeneration*, *13*(1), 66. https://doi.org/10.1186/s13024-018-0298-9

Grosser, T., Yu, Y., & Fitzgerald, G. A. (2010). Emotion recollected in tranquility: Lessons learned from the COX-2 saga. *Annual Review of Medicine*, *61*, 17–33. https://doi.org/10.1146/annurev-med-011209-153129

Guerreiro, R., & Bras, J. (2015). The age factor in Alzheimer's disease. *Genome Medicine, 7*, 106. https://doi.org/10.1186/s13073-015-0232-5

Heneka, M. T., Carson, M. J., El Khoury, J., Landreth, G. E., Brosseron, F., Feinstein, D. L., Jacobs, A. H., Wyss-Coray, T., Vitorica, J., Ransohoff, R. M., Herrup, K., Frautschy, S. A., Finsen, B., Brown, G. C., Verkhratsky, A., Yamanaka, K., Koistinaho, J., Latz, E., Halle,

A., … Kummer, M. P. (2015). Neuroinflammation in Alzheimer's Disease. *The Lancet. Neurology*, *14*(4), 388–405. https://doi.org/10.1016/S1474-4422(15)70016-5

Hopperton, K. E., Mohammad, D., Trépanier, M. O., Giuliano, V., & Bazinet, R. P. (2018). Markers of microglia in post-mortem brain samples from patients with Alzheimer's disease: A systematic review. *Molecular Psychiatry*, *23*(2), 177–198. https://doi.org/10.1038/mp.2017.246

Huang, L.-K., Chao, S.-P., & Hu, C.-J. (2020). Clinical trials of new drugs for Alzheimer disease. *Journal of Biomedical Science*, *27*(1), 18. https://doi.org/10.1186/s12929-019-0609-7

Ismeurt, C., Giannoni, P., & Claeysen, S. (2020). *The 5×FAD mouse model of Alzheimer's disease* (pp. 207–221). https://doi.org/10.1016/B978-0-12-815854-8.00013-6

Jiang, J., & Dingledine, R. (2013). Prostaglandin receptor EP2 in the crosshairs of anti-inflammation, anti-cancer, and neuroprotection. *Trends in Pharmacological Sciences*, *34*(7), 413–423. https://doi.org/10.1016/j.tips.2013.05.003

Kamphuis, W., Middeldorp, J., Kooijman, L., Sluijs, J. A., Kooi, E.-J., Moeton, M., Freriks, M., Mizee, M. R., & Hol, E. M. (2014). Glial fibrillary acidic protein isoform expression in plaque related astrogliosis in Alzheimer's disease. *Neurobiology of Aging*, *35*(3), 492–510. https://doi.org/10.1016/j.neurobiolaging.2013.09.035

Kim, Y. S., Jung, H. M., & Yoon, B.-E. (2018). Exploring glia to better understand Alzheimer's disease. *Animal Cells and Systems*, *22*(4), 213–218. https://doi.org/10.1080/19768354.2018.1508498

Kinney, J. W., Bemiller, S. M., Murtishaw, A. S., Leisgang, A. M., Salazar, A. M., & Lamb, B. T. (2018). Inflammation as a central mechanism in Alzheimer's disease. *Alzheimer's &*

Dementia : Translational Research & Clinical Interventions, *4*, 575–590. https://doi.org/10.1016/j.trci.2018.06.014

Landel, V., Baranger, K., Virard, I., Loriod, B., Khrestchatisky, M., Rivera, S., Benech, P., & Féron, F. (2014). Temporal gene profiling of the 5XFAD transgenic mouse model highlights the importance of microglial activation in Alzheimer's disease. *Molecular Neurodegeneration*, *9*(1), 33. https://doi.org/10.1186/1750-1326-9-33

Lee, J. W., Lee, Y. K., Yuk, D. Y., Choi, D. Y., Ban, S. B., Oh, K. W., & Hong, J. T. (2008). Neuro-inflammation induced by lipopolysaccharide causes cognitive impairment through enhancement of beta-amyloid generation. *Journal of Neuroinflammation*, *5*(1), 37. https://doi.org/10.1186/1742-2094-5-37

Livak, K. J., & Schmittgen, T. D. (2001). Analysis of relative gene expression data using real-time quantitative PCR and the 2(-Delta Delta C(T)) Method. *Methods (San Diego, Calif.)*, *25*(4), 402–408. https://doi.org/10.1006/meth.2001.1262

Ma, M. W., Wang, J., Zhang, Q., Wang, R., Dhandapani, K. M., Vadlamudi, R. K., & Brann, D. W. (2017). NADPH oxidase in brain injury and neurodegenerative disorders. *Molecular Neurodegeneration*, *12*(1), 7. https://doi.org/10.1186/s13024-017-0150-7

Manji, Z., Rojas, A., Wang, W., Dingledine, R., Varvel, N. H., & Ganesh, T. (2019). 5xFAD mice display sex-dependent inflammatory gene induction during the prodromal stage of Alzheimer's disease. *Journal of Alzheimer's Disease : JAD*, *70*(4), 1259–1274. https://doi.org/10.3233/JAD-180678

Martin, E., & Delarasse, C. (2018). Complex role of chemokine mediators in animal models of Alzheimer's Disease. *Biomedical Journal*, *41*(1), 34–40. https://doi.org/10.1016/j.bj.2018.01.002

Medeiros, R., Prediger, R. D. S., Passos, G. F., Pandolfo, P., Duarte, F. S., Franco, J. L., Dafre, A. L., Giunta, G. D., Figueiredo, C. P., Takahashi, R. N., Campos, M. M., & Calixto, J. B. (2007). Connecting TNF-α Signaling Pathways to iNOS Expression in a Mouse Model of Alzheimer's Disease: Relevance for the Behavioral and Synaptic Deficits Induced by Amyloid β Protein. *Journal of Neuroscience*, *27*(20), 5394–5404. https://doi.org/10.1523/JNEUROSCI.5047-06.2007

Metaxas, A., & Kempf, S. J. (2016). Neurofibrillary tangles in Alzheimer's disease: Elucidation of the molecular mechanism by immunohistochemistry and tau protein phospho-proteomics. *Neural Regeneration Research*, *11*(10), 1579–1581. https://doi.org/10.4103/1673-5374.193234

Minghetti, L. (2004). Cyclooxygenase-2 (COX-2) in Inflammatory and Degenerative Brain Diseases. *Journal of Neuropathology & Experimental Neurology*, *63*(9), 901–910. https://doi.org/10.1093/jnen/63.9.901

Minhas, P. S., Latif-Hernandez, A., McReynolds, M. R., Durairaj, A. S., Wang, Q., Rubin, A., Joshi, A. U., He, J. Q., Gauba, E., Liu, L., Wang, C., Linde, M., Sugiura, Y., Moon, P. K., Majeti, R., Suematsu, M., Mochly-Rosen, D., Weissman, I. L., Longo, F. M., … Andreasson, K. I. (2021). Restoring metabolism of myeloid cells reverses cognitive decline in ageing. *Nature*, *590*(7844), 122–128. https://doi.org/10.1038/s41586-020-03160-0

Monastero, R. N., & Pentyala, S. (2017). Cytokines as Biomarkers and Their Respective Clinical Cutoff Levels. *International Journal of Inflammation*, *2017*, e4309485. https://doi.org/10.1155/2017/4309485

Nathan, C., Calingasan, N., Nezezon, J., Ding, A., Lucia, M. S., La Perle, K., Fuortes, M., Lin, M., Ehrt, S., Kwon, N. S., Chen, J., Vodovotz, Y., Kipiani, K., & Beal, M. F. (2005).

Protection from Alzheimer's-like disease in the mouse by genetic ablation of inducible nitric oxide synthase. *The Journal of Experimental Medicine*, *202*(9), 1163–1169. https://doi.org/10.1084/jem.20051529

Neumann, H., Kotter, M. R., & Franklin, R. J. M. (2009). Debris clearance by microglia: An essential link between degeneration and regeneration. *Brain*, *132*(2), 288–295. https://doi.org/10.1093/brain/awn109

Newcombe, E. A., Camats-Perna, J., Silva, M. L., Valmas, N., Huat, T. J., & Medeiros, R. (2018). Inflammation: The link between comorbidities, genetics, and Alzheimer's disease. *Journal of Neuroinflammation*, *15*(1), 276. https://doi.org/10.1186/s12974-018-1313-3

Oakley, H., Cole, S. L., Logan, S., Maus, E., Shao, P., Craft, J., Guillozet-Bongaarts, A., Ohno, M., Disterhoft, J., Van Eldik, L., Berry, R., & Vassar, R. (2006). Intraneuronal β-Amyloid Aggregates, Neurodegeneration, and Neuron Loss in Transgenic Mice with Five Familial Alzheimer's Disease Mutations: Potential Factors in Amyloid Plaque Formation. *The Journal of Neuroscience*, *26*(40), 10129–10140. https://doi.org/10.1523/JNEUROSCI.1202-06.2006

Oblak, A. L., Lin, P. B., Kotredes, K. P., Pandey, R. S., Garceau, D., Williams, H. M., Uyar, A., O'Rourke, R., O'Rourke, S., Ingraham, C., Bednarczyk, D., Belanger, M., Cope, Z. A., Little, G. J., Williams, S.-P. G., Ash, C., Bleckert, A., Ragan, T., Logsdon, B. A., … Lamb, B. T. (2021). Comprehensive Evaluation of the 5XFAD Mouse Model for Preclinical Testing Applications: A MODEL-AD Study. *Frontiers in Aging Neuroscience*, *13*. https://www.frontiersin.org/article/10.3389/fnagi.2021.713726

O'Brien, R. J., & Wong, P. C. (2011). Amyloid Precursor Protein Processing and Alzheimer's Disease. *Annual Review of Neuroscience, 34,* 185–204. https://doi.org/10.1146/annurev-neuro-061010-113613

Ojala, J., Alafuzoff, I., Herukka, S.-K., van Groen, T., Tanila, H., & Pirttilä, T. (2009). Expression of interleukin-18 is increased in the brains of Alzheimer's disease patients. *Neurobiology of Aging*, *30*(2), 198–209. https://doi.org/10.1016/j.neurobiolaging.2007.06.006

Passos, G. F., Figueiredo, C. P., Prediger, R. D. S., Pandolfo, P., Duarte, F. S., Medeiros, R., & Calixto, J. B. (2009). Role of the Macrophage Inflammatory Protein-1α/CC Chemokine Receptor 5 Signaling Pathway in the Neuroinflammatory Response and Cognitive Deficits Induced by β-Amyloid Peptide. *The American Journal of Pathology*, *175*(4), 1586–1597. https://doi.org/10.2353/ajpath.2009.081113

Rojas, A., Ganesh, T., Wang, W., Wang, J., & Dingledine, R. (2020). A rat model of organophosphate-induced status epilepticus and the beneficial effects of EP2 receptor inhibition. *Neurobiology of Disease*, *133,* 104399. https://doi.org/10.1016/j.nbd.2019.02.010

Rubio-Perez, J. M., & Morillas-Ruiz, J. M. (2012). A Review: Inflammatory Process in Alzheimer's Disease, Role of Cytokines. *The Scientific World Journal*, *2012,* e756357. https://doi.org/10.1100/2012/756357

Savonenko, A., Munoz, P., Melnikova, T., Wang, Q., Liang, X., Breyer, R. M., Montine, T. J., Kirkwood, A., & Andreasson, K. (2009). Impaired cognition, sensorimotor gating, and hippocampal long-term depression in mice lacking the prostaglandin E2 EP2 receptor. *Experimental Neurology*, *217*(1), 63–73. https://doi.org/10.1016/j.expneurol.2009.01.016

Sheng, J. G., Bora, S. H., Xu, G., Borchelt, D. R., Price, D. L., & Koliatsos, V. E. (2003). Lipopolysaccharide-induced-neuroinflammation increases intracellular accumulation of amyloid precursor protein and amyloid beta peptide in APPswe transgenic mice. *Neurobiology of Disease*, *14*(1), 133–145. https://doi.org/10.1016/s0969-9961(03)00069-x

Simon, L. S. (1999). Role and regulation of cyclooxygenase-2 during inflammation. *The American Journal of Medicine*, *106*(5B), 37S-42S. https://doi.org/10.1016/s0002-9343(99)00115-1

Su, F., Bai, F., & Zhang, Z. (2016). Inflammatory Cytokines and Alzheimer's Disease: A Review from the Perspective of Genetic Polymorphisms. *Neuroscience Bulletin*, *32*(5), 469–480. https://doi.org/10.1007/s12264-016-0055-4

Takahashi, K., Rochford, C. D. P., & Neumann, H. (2005). Clearance of apoptotic neurons without inflammation by microglial triggering receptor expressed on myeloid cells-2. *The Journal of Experimental Medicine*, *201*(4), 647–657. https://doi.org/10.1084/jem.20041611

Tan, C.-C., Yu, J.-T., & Tan, L. (2014). Biomarkers for Preclinical Alzheimer's Disease. *Journal of Alzheimer's Disease*, *42*(4), 1051–1069. https://doi.org/10.3233/JAD-140843

Tuppo, E. E., & Arias, H. R. (2005). The role of inflammation in Alzheimer's disease. *The International Journal of Biochemistry & Cell Biology*, *37*(2), 289–305. https://doi.org/10.1016/j.biocel.2004.07.009

Ulland, T. K., & Colonna, M. (2018). TREM2—A key player in microglial biology and Alzheimer disease. *Nature Reviews Neurology*, *14*(11), 667–675. https://doi.org/10.1038/s41582-018-0072-1

Vérité, J., Page, G., Paccalin, M., Julian, A., & Janet, T. (2018). Differential chemokine expression under the control of peripheral blood mononuclear cells issued from Alzheimer's

patients in a human blood brain barrier model. *PLOS ONE*, *13*(8), e0201232. https://doi.org/10.1371/journal.pone.0201232

Verkhratsky, A., Olabarria, M., Noristani, H. N., Yeh, C.-Y., & Rodriguez, J. J. (2010). Astrocytes in Alzheimer's disease. *Neurotherapeutics*, *7*(4), 399–412. https://doi.org/10.1016/j.nurt.2010.05.017

Wang, P., Guan, P.-P., Wang, T., Yu, X., Guo, J.-J., & Wang, Z.-Y. (2014). Aggravation of Alzheimer's disease due to the COX-2-mediated reciprocal regulation of IL-1β and Aβ between glial and neuron cells. *Aging Cell*, *13*(4), 605–615. https://doi.org/10.1111/acel.12209

Wang, S., Mustafa, M., Yuede, C. M., Salazar, S. V., Kong, P., Long, H., Ward, M., Siddiqui, O., Paul, R., Gilfillan, S., Ibrahim, A., Rhinn, H., Tassi, I., Rosenthal, A., Schwabe, T., & Colonna, M. (2020). Anti-human TREM2 induces microglia proliferation and reduces pathology in an Alzheimer's disease model. *Journal of Experimental Medicine*, *217*(9), e20200785. https://doi.org/10.1084/jem.20200785

Wang, W.-Y., Tan, M.-S., Yu, J.-T., & Tan, L. (2015). Role of pro-inflammatory cytokines released from microglia in Alzheimer's disease. *Annals of Translational Medicine*, *3*(10), 7–7. https://doi.org/10.3978/j.issn.2305-5839.2015.03.49

Weggen, S., & Beher, D. (2012). Molecular consequences of amyloid precursor protein and presenilin mutations causing autosomal-dominant Alzheimer's disease. *Alzheimer's Research & Therapy*, *4*(2), 9. https://doi.org/10.1186/alzrt107

Wilcock, D. M., Gordon, M. N., & Morgan, D. (2006). Quantification of cerebral amyloid angiopathy and parenchymal amyloid plaques with Congo red histochemical stain. *Nature Protocols*, *1*(3), 1591–1595. https://doi.org/10.1038/nprot.2006.2770

Wu, C., Scott, J., & Shea, J.-E. (2012). Binding of Congo Red to Amyloid Protofibrils of the Alzheimer Aβ9–40 Peptide Probed by Molecular Dynamics Simulations. *Biophysical Journal*, *103*(3), 550–557. https://doi.org/10.1016/j.bpj.2012.07.008

Wyss-Coray, T. (2006). Inflammation in Alzheimer disease: Driving force, bystander or beneficial response? *Nature Medicine*, *12*(9), 1005–1015. https://doi.org/10.1038/nm1484

Yeo, I. J., Yun, J., Son, D. J., Han, S.-B., & Hong, J. T. (2020). Antifungal drug miconazole ameliorated memory deficits in a mouse model of LPS-induced memory loss through targeting iNOS. *Cell Death & Disease*, *11*(8), 1–14. https://doi.org/10.1038/s41419-020-2619-5

Zhang, C., Wang, Y., Wang, D., Zhang, J., & Zhang, F. (2018). NSAID Exposure and Risk of Alzheimer's Disease: An Updated Meta-Analysis From Cohort Studies. *Frontiers in Aging Neuroscience*, *10*, 83. https://doi.org/10.3389/fnagi.2018.00083

Zhu, M., Allard, J. S., Zhang, Y., Perez, E., Spangler, E. L., Becker, K. G., & Rapp, P. R. (2014). Age-Related Brain Expression and Regulation of the Chemokine CCL4/MIP-1A in APP/PS1 Double-Transgenic Mice. *Journal of Neuropathology & Experimental Neurology*, *73*(4), 362–374. https://doi.org/10.1097/NEN.0000000000000060

Zuena, A. R., Casolini, P., Lattanzi, R., & Maftei, D. (2019). Chemokines in Alzheimer's Disease: New Insights Into Prokineticins, Chemokine-Like Proteins. *Frontiers in Pharmacology*, *10*. https://www.frontiersin.org/article/10.3389/fphar.2019.00622